RESEARCH ARTICLE

Mechanistic Insights and Engineering Strategies for Wellbore Integrity Control in Polar Permafrost Reservoirs

Xiaohui Zhou[1,*], **Feiran Yang**[1], **Zhen Chen**[1] and **Yinao Su**[2]

[1] School of Energy Equipment Manufacturing, Dongying Vocational College, Dongying 257100, China
[2] Research Institute of Petroleum Exploration and Development, Beijing 100083, China

Abstract

Permafrost is typical temperature-sensitive sediment, and geo-mechanical issues such as wellbore collapse and sand production are prone to occur during the oil and gas development. Therefore, it is crucial to elucidate the patterns and mechanisms of wellbore instability throughout the drilling process and to develop/propose effective control strategies. In this study, based on sensitivity analysis of wellbore stability, a method for determining the safe windows of drilling fluid temperature, density, and salinity was proposed, along with corresponding measures for preventing wellbore collapse. The investigation results indicate that the collapse of sediments around the wellbore was primarily distributed within an elliptical region oriented along the direction of the minimum horizontal principal stress. Furthermore, the worsening of wellbore collapse gradually slows as drilling operation progresses, and the final borehole enlargement rate corresponding to the default investigation case reaches 89.84%. Sensitivity analysis showed that higher drilling fluid temperature, lower density, and elevated salinity all negatively affect wellbore stability. However, wellbore stability is easier to maintain when the permafrost has high initial ice saturation, low stress difference, and shallow burial depth. Ultimately, the safe mud temperature, density, and salinity windows derived from the wellbore stability simulations are beneficial for accurately controlling wellbore stability within the required range.

Keywords: wellbore integrity, numerical simulation, permafrost, wellbore collapse, engineering optimization.

1 Introduction

At present, the development and utilization of emerging sustainable energy sources, such as solar and geothermal energy, are gradually gaining attention [1]. Nevertheless, fossil fuels, including oil, natural gas and coal, will continue to serve as the important energy sources for supporting rapid economic and social development for the foreseeable future. However, the decline in production capacity of mature oil fields in central and eastern China has driven the expansion of exploration and production operation into unconventional oil and gas resources, such as polar permafrost area [2–4]. According to USGS (United States Geological Survey), unexplored oil and

Submitted: 15 December 2025
Accepted: 22 April 2026
Published: 29 April 2026

Vol. 2, **No.** 2, 2026.
10.62762/RS.2025.816374

***Corresponding author:**
Xiaohui Zhou
339762462@qq.com, b17020052@s.upc.edu.cn

Citation
Zhou, X., Yang, F., Chen, Z., & Su, Y. (2026). Mechanistic Insights and Engineering Strategies for Wellbore Integrity Control in Polar Permafrost Reservoirs. *Reservoir Science*, 2(2), 126–150.

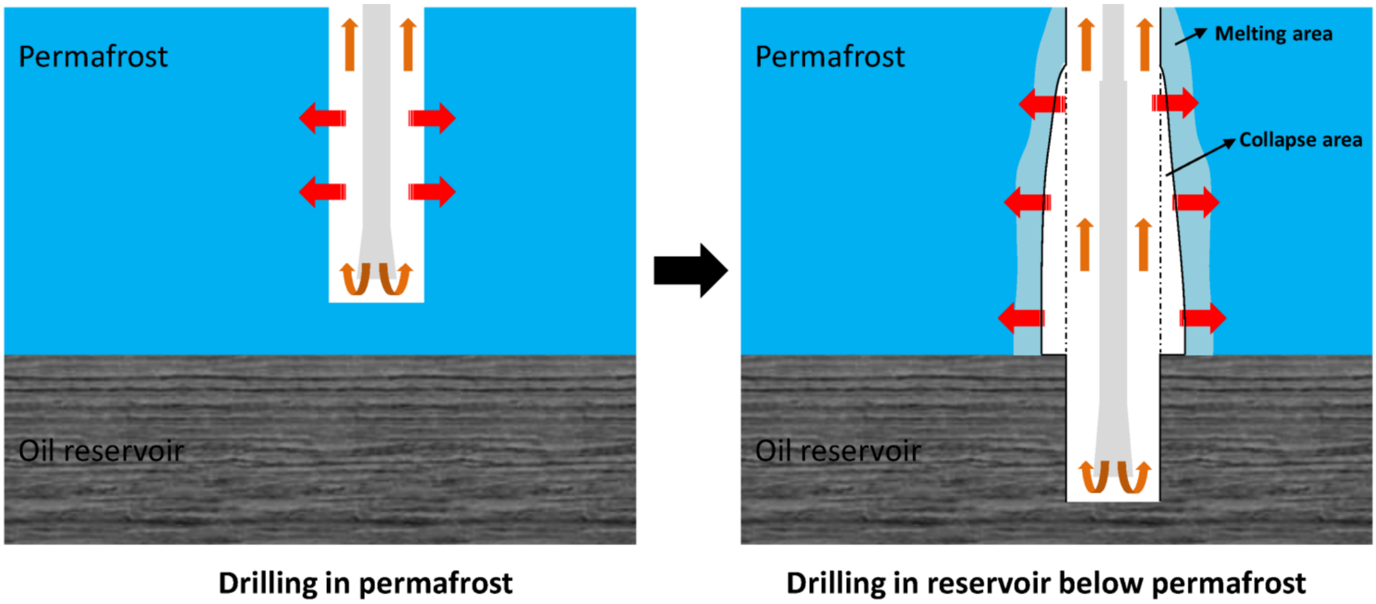

Figure 1. Schematic diagram of wellbore collapse in permafrost region.

natural gas reserves in the Arctic region account for 13% and 30% of the global totals, respectively [5]. The total oil and gas reserves amount to as much as 400 billion barrels of crude oil. Against the background of rapid global economic development and increasing energy constraints, the strategic significance of Arctic oil and gas resources has become increasingly prominent [6–8]. At present, research and application related to the development of oil and gas resources in polar permafrost regions remain largely dominated by Arctic Rim countries such as Canada, Norway, and Russia [9, 10]. Although China has made notable progress in these areas over the past decade, investigations on wellbore stability prediction and control technologies in permafrost remain in its early stage [11]. This has adversely affected the safe and efficient development of oil and gas resources in polar permafrost regions for China. Therefore, in-depth investigation on polar drilling is of substantial significance for ensuring the implementation of arctic and subarctic oil and gas development.

In the Arctic, permafrost may extend to depths exceeding 1,000 meters [8]. It is essential for the development and extraction of oil and gas in polar region to drill through this formation [12, 13]. However, the permafrost is a typical temperature-sensitive formation, and its susceptibility to melting leads to more severe sediment instability and wellbore deformation during drilling operation compared to conventional reservoirs [14, 15]. Just as shown in Figure 1, the high-temperature drilling fluid circulating in the annulus transfers heat to the surrounding permafrost during drilling operation, inevitably causing ice melting and a reduction in sediment strength. Combined with stress concentration, severe plastic deformation can occur in the surrounding sediment, potentially resulting in wellbore collapse and sediment damage [16–18]. Furthermore, the pronounced creep characteristics of permafrost can intensify borehole enlargement and collapse, thereby further hindering the effective exploitation of polar oil and gas resources [19, 20]. In addition, wellbore instability tends to intensify with longer drilling duration and deeper wellbore penetration.

Currently, investigations into borehole stability in permafrost are far less advanced than those for conventional reservoirs, with limited analyses addressing borehole deformation during drilling in permafrost. Although existing studies have offered valuable insights into mechanisms of wellbore instability, a number of shortcomings and limitations still remain [21]. To begin with, both the complexity of the mathematical models and the challenges of numerical solutions make fully coupled multi-physics simulations difficult. Thus, many existing studies have solved models through sequential coupling strategy [22, 23]. However, such simplifications inevitably introduce deviations in the simulation results, which may affect the formulation and implementation of corresponding engineering measures and strategies. What is more, the mechanisms and synergistic effects of multiple influencing factors have not been systematically

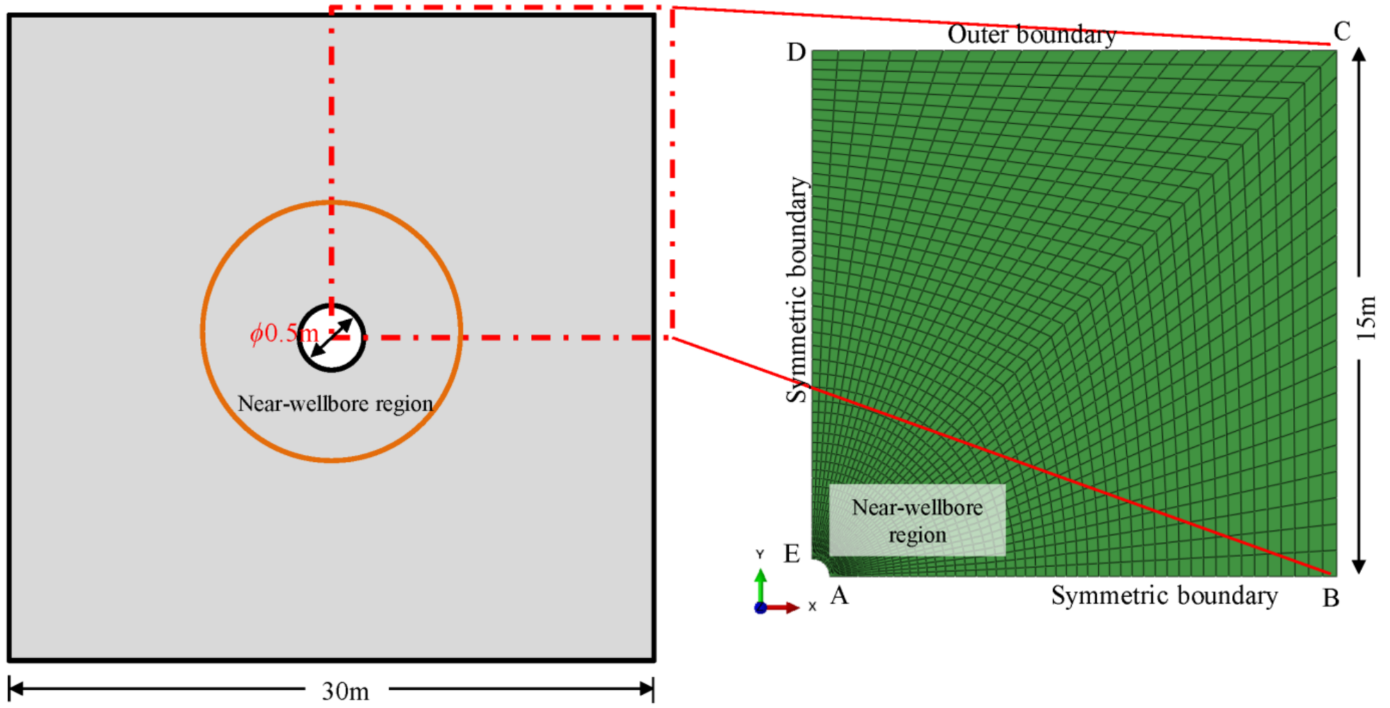

Figure 2. Geometric model used for simulation of wellbore stability.

Table 1. Configuration of boundary conditions and loads.

Boundary	1st step		2nd step	
	Type	Value	Type	Value
Borehole AE	Fixed temperature boundary	/	Fixed temperature boundary	Drilling fluid temperature
	Fixed pore-pressure boundary	/	Fixed pore-pressure boundary	Drilling fluid pressure
	Mechanical boundary	$Ux=Uy=Uz=0$	Mechanical boundary	Bottom-hole pressure
AB and ED	Fixed temperature boundary	/	Fixed temperature boundary	/
	Fixed pore-pressure boundary	/	Fixed pore-pressure boundary	/
	Mechanical boundary	*Fix normal displacement*	Mechanical boundary	*Fix normal displacement*
BC and CD	Fixed temperature boundary	/	Fixed temperature boundary	Initial sediment temperature
	Fixed pore-pressure boundary	/	Fixed pore-pressure boundary	Initial pore pressure
	Mechanical boundary	*Fix normal displacement*	Mechanical boundary	Initial horizontal stresses

analyzed, leading to a limited understanding of stability evolution in permafrost [24–26]. This, to some extent, constrains the use of simulation results for regulating and managing wellbore instability. Last but not least, existing models have largely neglected the potential chemical reactions, such as ice melting [27, 28]. This may compromise the accurate mathematical representation of the thermo–hydraulic-mechanical–chemical coupling mechanism around the wellbore. Overcoming these limitations to achieve an accurate characterization of the wellbore instability process is of great significance for enabling precise control of wellbore stability during drilling in permafrost [29, 30].

Based on these limitations, this study investigates characteristics of ice melting range, physical parameters, and yield area in the near-wellbore region were studied. Simultaneously, the effects of geological factors, such as ice saturation, and engineering factors, such as drilling fluid density, on wellbore collapse and instability were analyzed. The corresponding influencing mechanisms were investigated from the perspectives of stress distribution, physical property variations, and ice melting. By synthesizing the quantitative results of wellbore instability obtained above, key engineering parameters—including drilling fluid density, temperature, and salinity—were optimized and designed.

2 Geometric Model for Wellbore Stability Analysis

2.1 Model Geometry

Figure 2 presents the geometric model used for the numerical simulation of wellbore stability in permafrost. To balance computational efficiency with simulation accuracy, the model is developed as an

Table 2. Initial conditions in simulation.

Objective	Type	Value
Whole model	Initial stress	In-situ stresses (i.e., σ_{v0}, σ_{H0} and σ_{h0})
	Initial temperature	Initial sediment temperature, T_{i0}
	Initial fluid saturation	Initial saturation of gas, ice and water (i.e., S_{i0}, S_{w0} and S_{g0})
	Initial pressure	Initial pore pressure in sediment, P_{p10}

axisymmetric two-dimensional configuration, thereby effectively reducing the required mesh density. As illustrated in Figure 2, the arc AE in the lower-left part of the model denotes the borehole formed by the drill bit, with a radius of 0.25 m. The boundary length is 15 m (60 times the wellbore size), allowing boundary effect to be effectively avoided. The boundaries AB and DE are axisymmetric, and the full-model results can be obtained through mirror symmetry. In addition, boundaries BC and CD form the model's outer boundary, on which temperature and pore-pressure boundary conditions must be applied during the simulation. Since the disturbance induced by drilling operations is confined to a limited area around wellbore, the 5.0-m region surrounding the wellbore is defined as the near-wellbore region. Meanwhile, the elements in this region (the near-wellbore region) are refined to be smaller than those away from the wellbore. After mesh refinement, the model contains a total of 43,200 CPE4P elements, of which about 74% are located within the near-wellbore region.

The simulation includes two analysis steps with different functions. The first analysis step aims to establish the initial state of the permafrost, which serves as the foundation for simulating wellbore collapse. The second analysis step is the main one, which controls the main simulation process. Based on the reservoir depth and the purposes of the two analysis steps, the simulation times of both steps are defined as 1 s and 3 days, respectively. When building the geometric model, the permafrost region corresponding to the wellbore is pre-segmented using the "Partition" function. It should be emphasized that no interaction exists between this permafrost region (i.e., wellbore) and the remaining region. In addition, the activation and deactivation of the elements within wellbore across the two analysis steps must be controlled through the "Model Change" function. During the first analysis step, the investigation model consists of an intact rectangular domain measuring 15 m × 15 m. At this analysis step, the "Model Change" function is inactive, indicating that the elements within wellbore are still part of the model in their original state. When the simulation proceeds to the second analysis step, the Model Change function is activated, and the corresponding elements in wellbore region are removed from the model. On this basis, Table 1 summarizes the configuration of boundary conditions and loads applied in the two analysis steps of the simulation respectively.

Furthermore, four initial conditions must be specified for the wellbore stability simulation in permafrost, as summarized in Table 2.

2.2 Basic Data

The fundamental parameters required for simulation are equally critical to the numerical analysis of wellbore stability. Therefore, the key parameters adopted for the simulation of wellbore stability in permafrost are summarized in Table 3.

Table 3. Basic data for simulation of wellbore stability in permafrost [1, 12].

Parameter	Value	Unit
Model size	15	m
Depth of wellbore	500	m
Initial porosity	42.46	%
Thermal conductivity	1.4	W/(m·K)
Ice saturation	30.00	%
Reservoir temperature	-8.0	℃
Initial cohesion	1.25	MPa
Initial internal friction angle	23.5	°
Initial elastic modulus	500	MPa
Initial Poisson's ratio	0.28	-
Reservoir pore pressure	5.0	MPa
drilling fluid density	1014.3	kg/m^3
Specific heat of sediment	1900	J/(kg·K)
water saturation	25.0	%
Density of reservoir skeleton	2500	g/cm^3
Absolute permeability	4.00	mD
Maximum horizontal principal stress	4.60	MPa
Minimum horizontal principal stress	3.06	MPa
Vertical principal stress	6.15	MPa
Drilling fluid temperature	30.0	℃
Relative mud density	0.98	-
Wellbore radius	0.25	m
Drilling fluid salinity	20	g/L

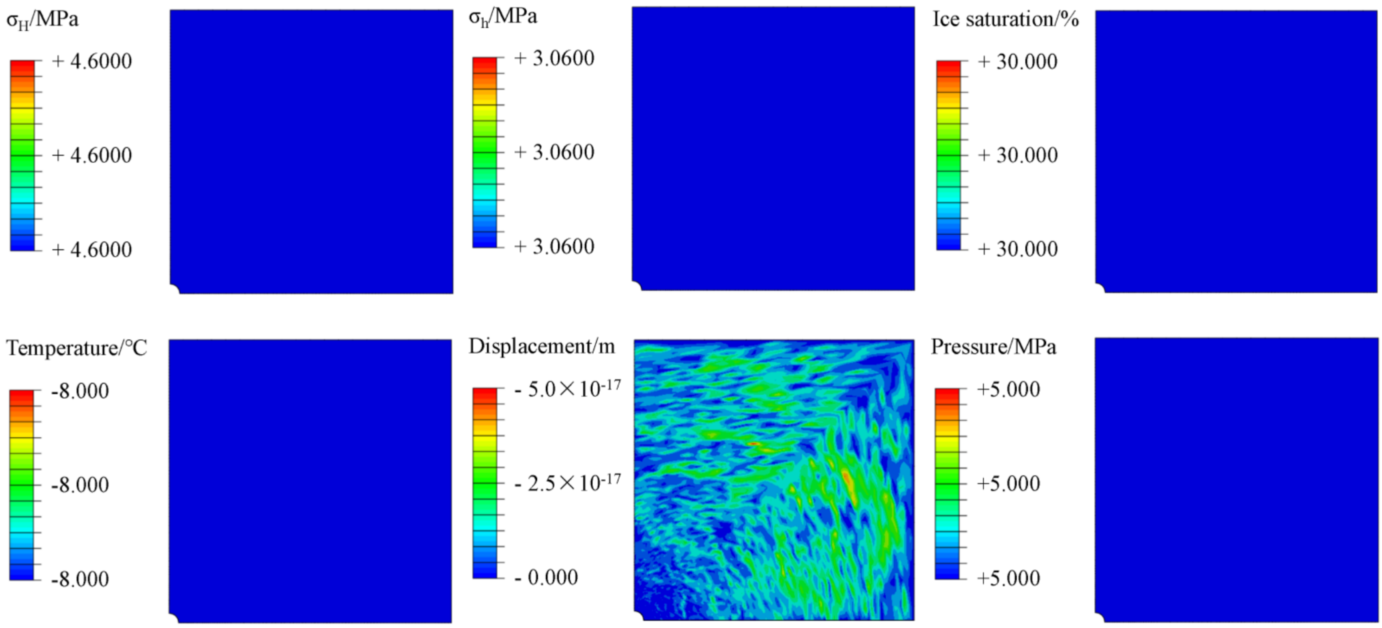

Figure 3. Initial distribution of various physical parameters in the model.

2.3 Evolutionary Features of Wellbore Instability

As noted earlier, the purpose of the first analysis step (i.e., the Geostatic step) is to establish the initial state of the sediment within the model, thereby providing the requisite initial conditions for the subsequent wellbore stability simulation.

Figure 3 presents the spatial distributions of the various physical parameters within the model. As shown in Figure 3, all reservoir characteristic parameters exhibit uniform spatial distributions consistent with the initial values, with the exception of the sediment deformation. For instance, the maximum and minimum horizontal principal stresses throughout the model are 4.60 MPa and 3.06 MPa, respectively, which are fully consistent with the corresponding values listed in Table 3. In addition, the spatial distributions of ice saturation, temperature, and pore pressure within the model exhibit the same uniform patterns and characteristics. Besides, there are similar distribution patterns and characteristics for ice saturation, temperature, and pore pressure distribution. In Figure 3, the sediment deformation within the model is on the order of 10^{-17} m, a magnitude that can be directly ignored. This "stressed yet strain-free" condition can therefore be adopted as the initial state for the wellbore stability simulation in the second analysis step.

In this study, the equivalent plastic strain (PEEQ) was adopted as parameter to determine wellbore instability. In this study, PEEQ≥0.00 is defined as the threshold for local structural failure (collapse). The borehole enlargement rate is determined by the area of the region where PEEQ exceeds this threshold, expressed as $rbe = (A_{col} - A_{inb})/A_{inb} \times 100\%$. Where, Acol is the area of the region where PEEQ is greater than 0, and Ainb is the cross-sectional area of wellbore. Obviously, both larger equivalent plastic strain values and more extensive distribution of positive PEEQ indicate a more severe case of wellbore instability. Figure 4 presents the distributions of equivalent plastic strain (i.e., PEEQ) in the near-wellbore region at various drilling times. The results shown in Figure 4 indicate that the wellbore instability occurring during drilling operations in permafrost exhibits a pronounced temporal dependence. As observed in Figure 4, collapse first occurs at the two intersection points of wellbore with the vertical plane passing through the minimum horizontal principal stress at approximately 0.2s after drilling operation begins. At this time, both the severity and range of the collapse are limited, confined to these two collapse points. If corresponding engineering measures are taken at this time, the stability of wellbore will not be threatened. However, as the drilling operation progresses, the collapse area gradually expand outward from the two initial collapse points in both radial and circumferential directions. Although the radial and circumferential expansion of the collapse area occurs simultaneously throughout the drilling process, there is a clear difference in the drilling cycle dominated by these two expansion modes. In the initial 12 hours of the drilling operation, the expansion of the collapse area occurs predominantly in the circumferential direction.

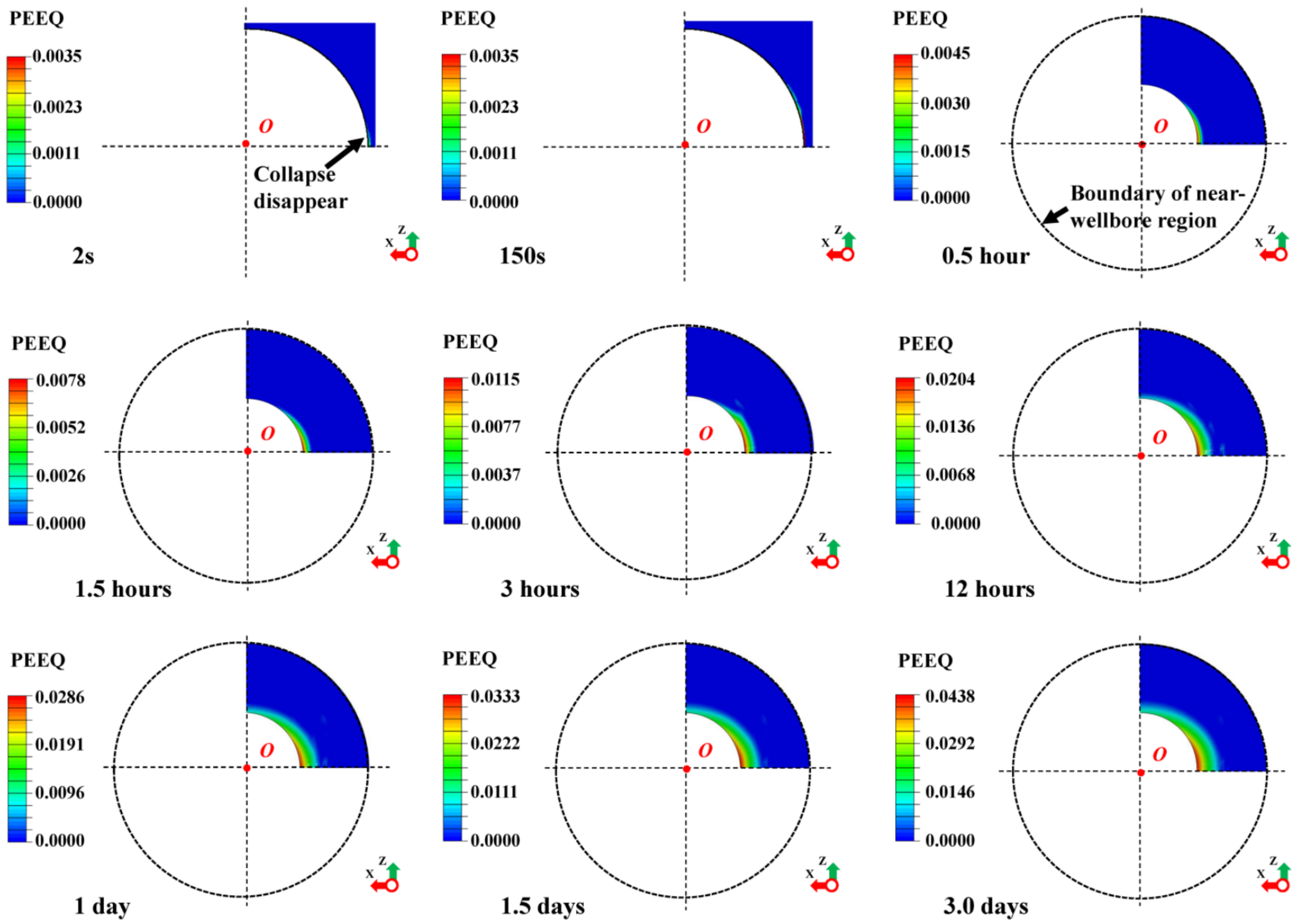

Figure 4. Evolution distribution of equivalent plastic strain within the near-wellbore region throughout the drilling process.

At this stage, the collapse area exhibits a rapid and pronounced expansion. However, once the collapse areas on both sides closed at 12 hours, radial expansion begins to dominate. Upon entering this stage, the expansion of the collapse area gradually slows down. The reason is that the rate of ice melting around the wellbore decreases over time. At the end of the drilling operation, the collapse area surrounding the wellbore exhibits an elliptical distribution. Of course, not all collapse area around wellbore are a complete ellipse under all drilling conditions.

The evolutionary pattern shown in Figure 4 can provide critical guidance for field operations. Specifically, the elliptical distribution of the collapse area, oriented along the minimum horizontal principal stress, suggests that directional well trajectories should ideally be aligned with the maximum horizontal principal stress direction to minimize the non-uniform stress concentration and subsequent borehole enlargement. Furthermore, the rapid circumferential expansion observed within the first 12 hours highlights a critical window for casing operations. To ensure wellbore integrity and avoid the detrimental effects of secondary radial expansion driven by ice melting, casing should be inserted and cemented as soon as possible after the target depth is reached, preferably before the transition from circumferential to radial dominance in collapse evolution.

Under the default drilling parameters, the collapse region finally expands to 89.84% of the original wellbore cross-sectional area, indicating severe instability. This parameter is designated as the borehole enlargement rate, and wellbore stability is quantified by it in the following sensitivity analysis.

3 Effect of Geological Factors on Wellbore Stability

In this section, the influence of three geological factors, namely initial ice saturation, in-situ stress, and model depth, on wellbore stability during drilling in permafrost was analyzed. Although these factors

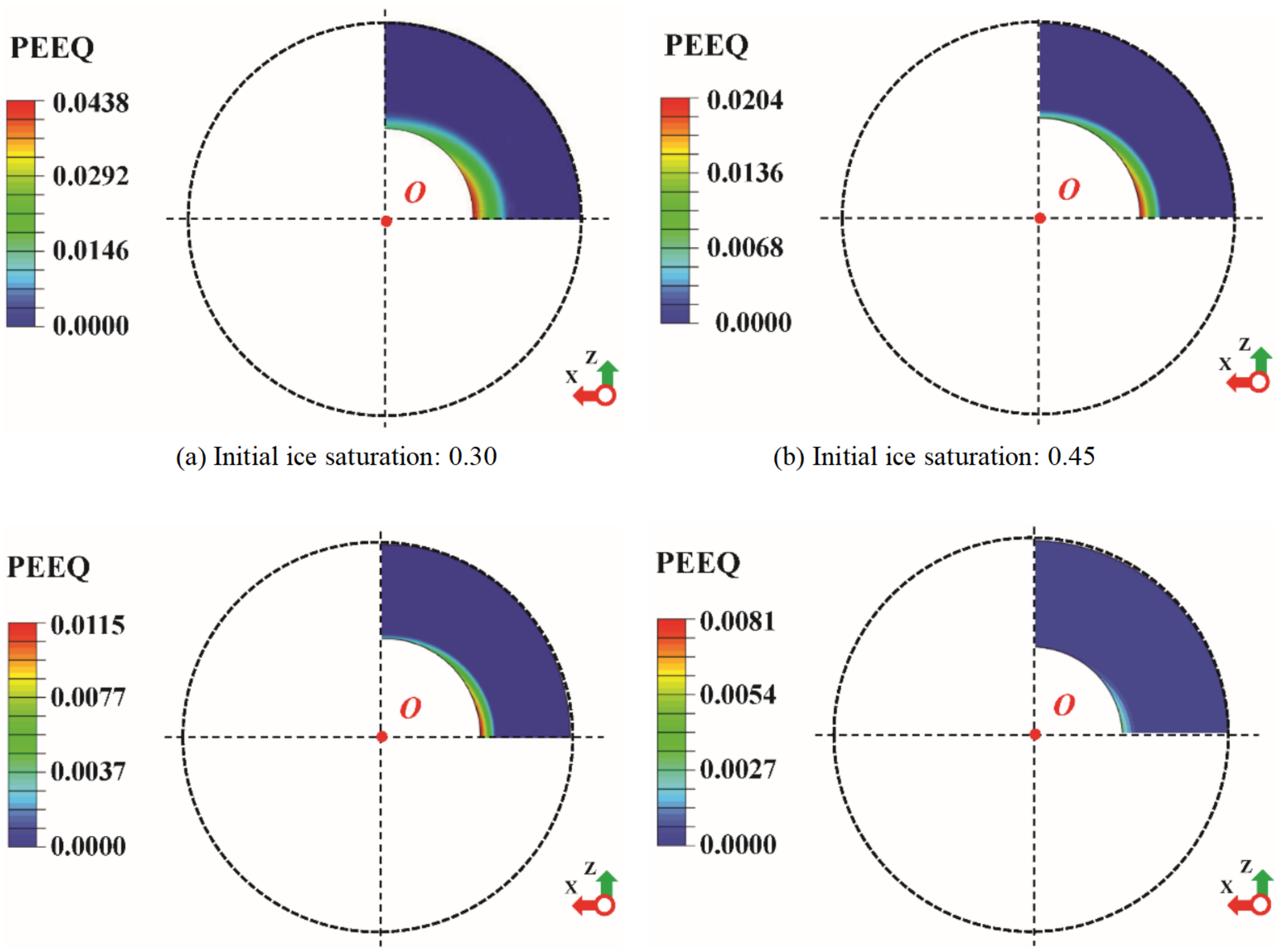

(a) Initial ice saturation: 0.30 (b) Initial ice saturation: 0.45

(c) Initial ice saturation: 0.60 (d) Initial ice saturation: 0.75

Figure 5. Effect of initial ice saturation on wellbore stability.

cannot be artificially controlled, in-depth investigation can clarify their influence mechanisms and supports the design and optimization of drilling operation in permafrost.

3.1 Initial Ice Saturation

Ice saturation modifies the mechanical behavior of permafrost, which in turn reshapes the stress field around the wellbore and may trigger its instability or collapse [31, 32]. Therefore, differences in initial ice saturation have a pronounced impact on wellbore stability during drilling in permafrost. To evaluate the influence of ice saturation, simulations were conducted for initial values of 0.30, 0.45, 0.60, and 0.75, while the other model parameters followed the settings provided in Table 3.

The PEEQ distribution nephogram in the near-wellbore region for initial ice saturations of 0.30, 0.45, 0.60, and 0.75 are shown in Figure 5. From Figure 5, it can be clearly seen that higher initial ice saturation in permafrost leads to an extensive reduction in the range of the potential collapse area surrounding the wellbore. However, when the initial ice saturation is lower than 0.60, the plastic yield region (i.e., potential collapse area) around wellbore is fully interconnected. For initial ice saturation above 0.60, the plastic yield region no longer interconnects and is limited to a small region around wellbore in the direction of the minimum principal stress. Additionally, as revealed in Figure 5, the intensity of plastic yielding (i.e., PEEQ value) decreases markedly as the initial ice saturation increases, and the stability of the wellbore stability is significantly improved. The results presented in Figure 5 provide only a qualitative indication of how initial ice saturation affects wellbore stability during drilling in permafrost. To provide a more reliable theoretical basis for drilling engineering design, the further quantitative analysis of wellbore stability is required. Thus, the relationship curve between borehole enlargement rate and initial ice saturation is displayed in Figure 6. As evidenced by Figure 6, the sensitivity of wellbore stability to initial ice saturation is substantially heightened in the low-saturation interval, whereas the effect diminishes as saturation increases. The point at which the influence begins to weaken is situated near an ice saturation of 0.50. As the initial ice saturation rises from 0.30 to 0.50, the borehole enlargement rate drops sharply from 89.84% to 33.82%, with a reduction of up to 56.02%. However, as the initial ice saturation increases from 0.50 to 0.80, the decline in the borehole enlargement rate is markedly attenuated, falling only from 33.82% to 8.83%. This transition point (i.e., ice saturation of 0.5) arises from a transformation of the skeleton support mode in permafrost. When the ice saturation exceeds 0.5, the skeleton support mode will change from a soil-particle-dominated mode to an ice-dominated mode. As the filling of pores by ice becomes saturated, its marginal contribution to sediment shear strength gradually decreases.

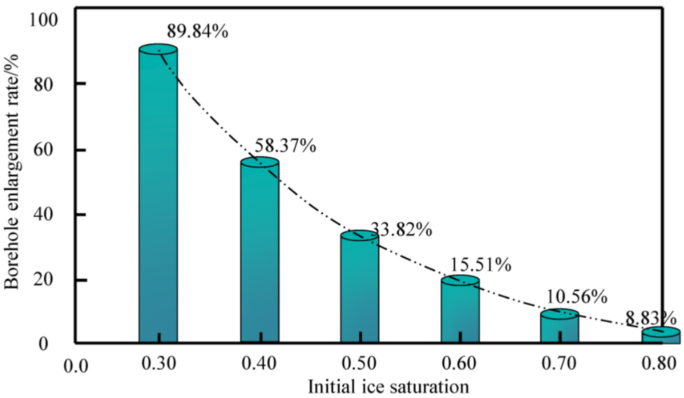

Figure 6. Effect of initial ice phase saturation on wellbore stability.

The influence mechanism of initial ice saturation on wellbore stability can be explored from two perspectives: (i) its effect on ice melting, and (ii) the associated variations in the stress state. To further explain the results presented in Figures 5 and 6, Figure 7 illustrates the evolution of the ice-melting range under various initial ice saturations. At low ice saturation, the ice cementation within the permafrost is weak, enabling rapid heat transfer from the high-temperature drilling fluid to the sediment and resulting in accelerated ice melting. For example, when the initial ice saturation is 0.30, the melting range of ice around wellbore is as wide as 32.54 cm (see Figure 7). For this case, the permafrost within the large-scale ice-melting region around wellbore was severely softened, leading to a marked reduction in mechanical strength. Therefore, the wellbore stability worsens, resulting in a larger borehole enlargement rate. Meanwhile, the mechanical strength of permafrost with low ice saturation is weak, making the skeleton are prone to particle rearrangement and plastic deformation after being disturbed by drilling operations. Moreover, in low-strength sediments, stress is released rapidly, which further aggravates borehole enlargement and collapse. As the initial ice saturation increases, permafrost strength is enhanced due to the strengthened ice cementation. Consequently, the structural integrity of the permafrost becomes more stable. Moreover, at high initial ice saturation, the expansion of the ice-melting region around wellbore was significantly restricted [33]. As illustrated in Figure 7, the width of the ice-melting region decreases to 6.84 cm when the initial ice saturation is 0.75. Under conditions of high ice saturation, the localized melting of ice and the limited range of stress concentration alleviate wellbore instability, thereby slowing down the reduction in borehole enlargement rate.

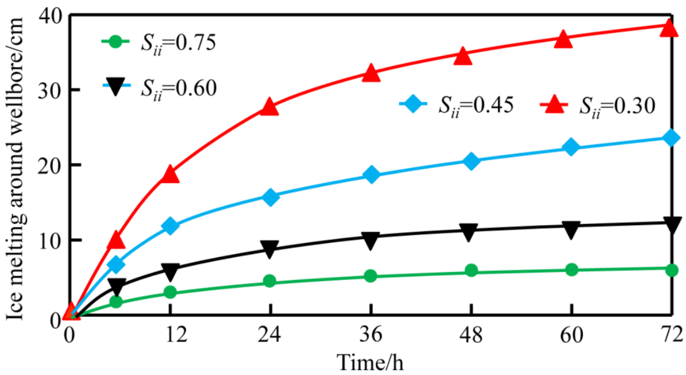

Figure 7. Range of ice melting around wellbore for different initial ice saturation in permafrost.

3.2 Difference Between in-situ Stresses

Wellbore stability analysis is essentially governed by mechanics, and the sediment stresses in the model play a critical role in determining the wellbore behavior [34, 35]. Thus, assessing the impact of in-situ stress is of considerable engineering significance for improving wellbore stability. Figure 8 illustrates the equivalent plastic strain distribution within the near-wellbore region for in-situ stress ratios of 1.15, 1.30, 1.45, and 1.60. In this work, the ratio—defined as the difference coefficient—denotes the ratio of the maximum horizontal principal stress to the minimum horizontal principal stress, and represented as $\chi = \sigma H/\sigma h$.

From the nephogram displayed in Figure 8, it can

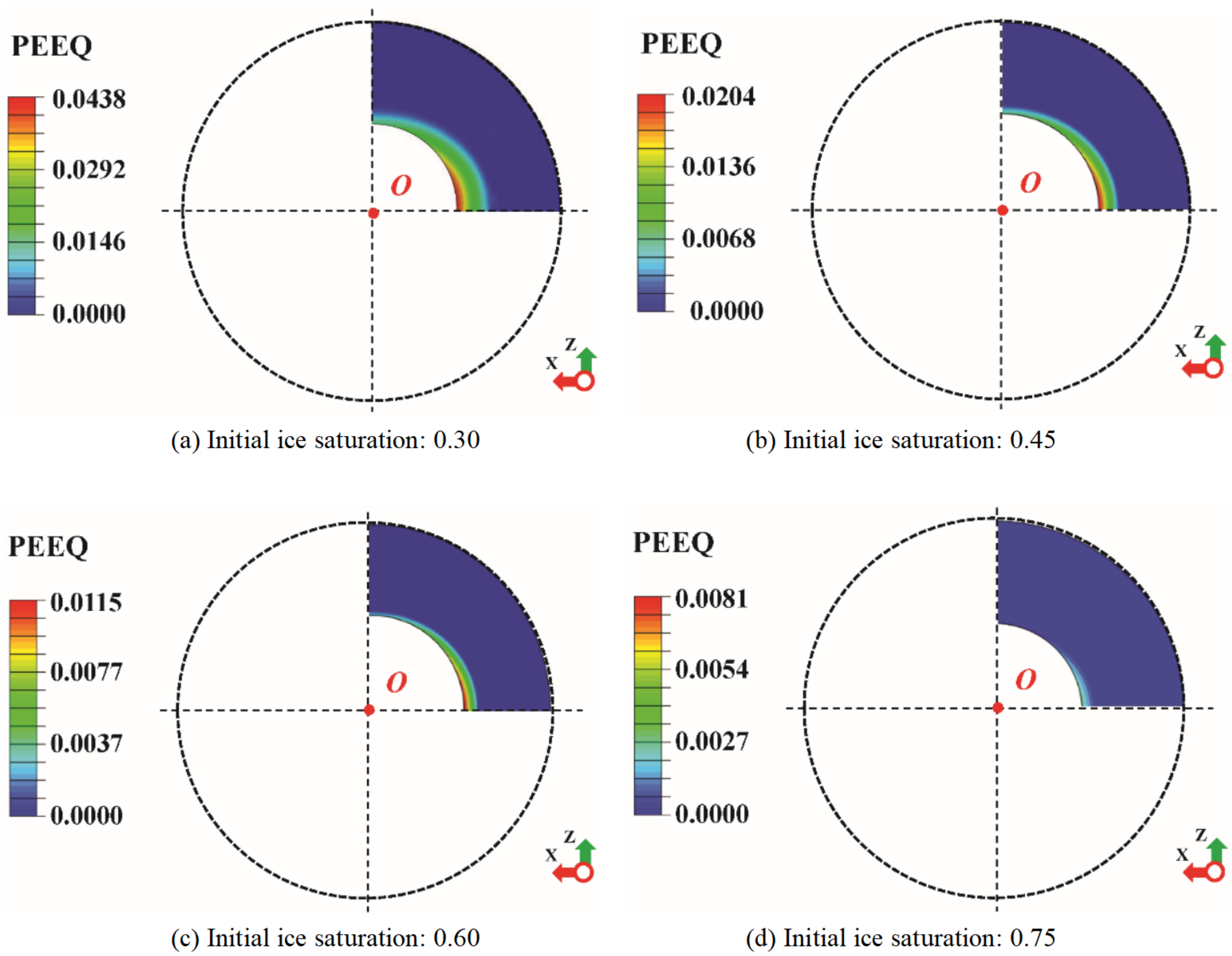

Figure 8. Effect of difference between in-situ stress components on wellbore stability.

be clearly seen that an increase in the difference between in-situ stresses can lead to a pronounced enlargement of the collapse area around wellbore. When the difference coefficient is low, such as $\chi = 1.15$, the potential collapse area around wellbore is small. For this case, the wellbore stability is good, with a borehole enlargement rate of 19.21%. As the stress difference increases, the collapse area around wellbore expands significantly, extending toward the right. This is because an increase in the difference between the in-situ stress components induces more pronounced stress concentration, causing sediment yielding over a larger area around wellbore [36, 37]. The borehole enlargement rate has increased to 89.84% when the difference coefficient is 1.45. When the difference coefficient reaches 1.60, the plastic yield area around wellbore nearly encompasses the entire wellbore, with the borehole enlargement rate reaching 125.72%. For these high difference coefficient conditions, the wellbore is critically unstable, with a high probability of uncontrollable borehole collapse.

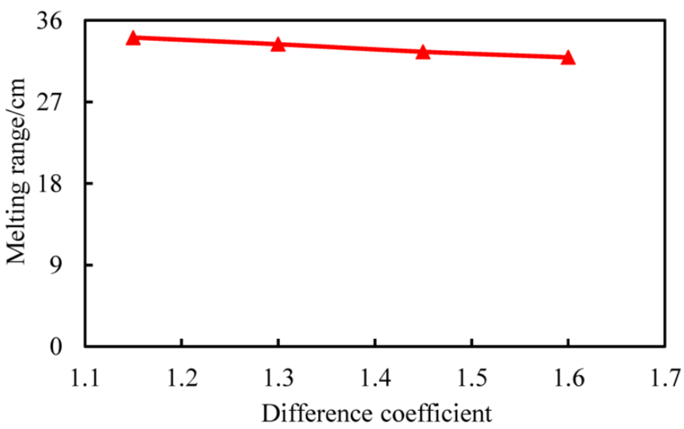

Figure 9. Effect of difference between in-situ stresses on ice melting around wellbore.

The difference in ice melting under different in-situ stresses is also an important potential factor affecting wellbore stability. Figure 9 presents the quantitative results for the ice melting range around wellbore under various in-situ stress conditions. As shown in Figure 9, although the melting ranges of ice around wellbore becomes slightly narrower with increasing difference between stress components, this reduction is minimal. As the difference coefficient increased from 1.15 to 1.60, the melting range of ice around the wellbore narrowed from 34.11 cm to 31.92 cm, corresponding to a reduction of only 2.19 cm. This slight variation in the melting range of the ice can be attributed to the pronounced reduction in sediment permeability when differential coefficient is high. This reduced permeability slows both heat transfer and fluid seepage, thereby diminishing the disturbance caused by drilling operations on the stability of ice within the near-wellbore region [38]. Nevertheless, this impact is weak. Therefore, the variation in ice melting induced by differences in in-situ stresses is not the primary factor governing the wellbore stability results shown in Figure 8.

3.3 Model Depth

Variations in the depth of permafrost can change factors such as temperature, pressure, and stress within the model, thereby influencing wellbore stability [39]. Before investigating the influence of permafrost depth on wellbore stability, it is first necessary to determine the possible depth distribution range of the permafrost layer. In Arctic region, the depth of permafrost typically ranges from several tens to several hundreds of meters. In some cold regions, the thickness of the permafrost layer can reach between 500 and 1000 meters [40]. For example, in regions such as Siberia and Alaska, the average permafrost thickness typically ranges from 300 to 500 m. When the surface temperature and geothermal gradient are assumed to be -15 °C and 2.8 °C/100 m, respectively, the maximum depth of the permafrost layer is determined to be 535.71 m. Based on this, wellbore stability was examined at permafrost depths of 125 m, 250 m, 375 m, and 500 m in this section. The corresponding nephogram and quantitative results were presented in Figure 10.

As shown in Figure 10, the range of PEEQ distribution around wellbore during drilling in the permafrost increases prominently with increasing model depth. This indicates that wellbore stability deteriorates as the depth of investigation model increases. For shallow permafrost, the temperature of the sediment itself is low, and the ice within the sediment remains naturally stable under such low-temperature conditions. In this case, most of the heat transferred from the high-temperature drilling fluid is consumed in raising the sediment temperature, and only a small portion is used for ice melting [41]. Therefore, in shallow permafrost conditions, the melting range of ice around the wellbore is extremely limited. When the model depth is 125 meters, the final range of ice melting within the near-wellbore region is only 2.43 cm (see Figure 11). Even when the model depth increases to 250 m, the melting range of ice in the permafrost around the wellbore is only 9.12 cm. Moreover, in shallow permafrost, the stresses in all directions are low, and the permafrost structure is comparatively stable. In this case, stress concentration around the wellbore is minimal, and wellbore stability can be maintained. When the model depth is located shallower than 168.4 m, no yield area develops in the sediment within the near-wellbore region, and the borehole enlargement rate is zero. Even when the model depth increases to 250 m, the borehole enlargement rate is only 7.86%. As the model depth increases, the sediment temperature gradually rises, and the heat transferred from the high-temperature drilling fluid is primarily consumed by the melting of the ice. When the model depth reaches 375 m and 500 m, the melting front extends to 17.86 cm and 32.54 cm from the wellbore, respectively. The melting of ice significantly reduces the strength of permafrost, and the wellbore is prone to plastic deformation or collapse. For the models with depths of 375 m and 500 m, the final borehole enlargement rates were 43.24% and 89.84%, respectively. It can be inferred that at deeper depths, wellbore collapse and instability will become more severe, and higher borehole enlargement rates will be presented.

Nevertheless, we can see from Figure 10 that the influence of permafrost depth on wellbore stability varies across different depth ranges. This effect strengthens with increasing depth, as illustrated and revealed by the slope of the curve in Figure 10. This is primarily because ice melting in permafrost becomes progressively easier as the depth increases. In particular, the influence of depth on wellbore stability arises from the coupled effects of the geothermal gradient and in-situ pressure. The high initial temperature at deeper depths promotes more rapid melting of ice and accelerates the expansion of the affected region. Meanwhile, the high-pressure environment intensifies the risk of shear failure in the ice-melted region, which results in a significant reduction in wellbore stability. Therefore, during the drilling process of permafrost, special attention

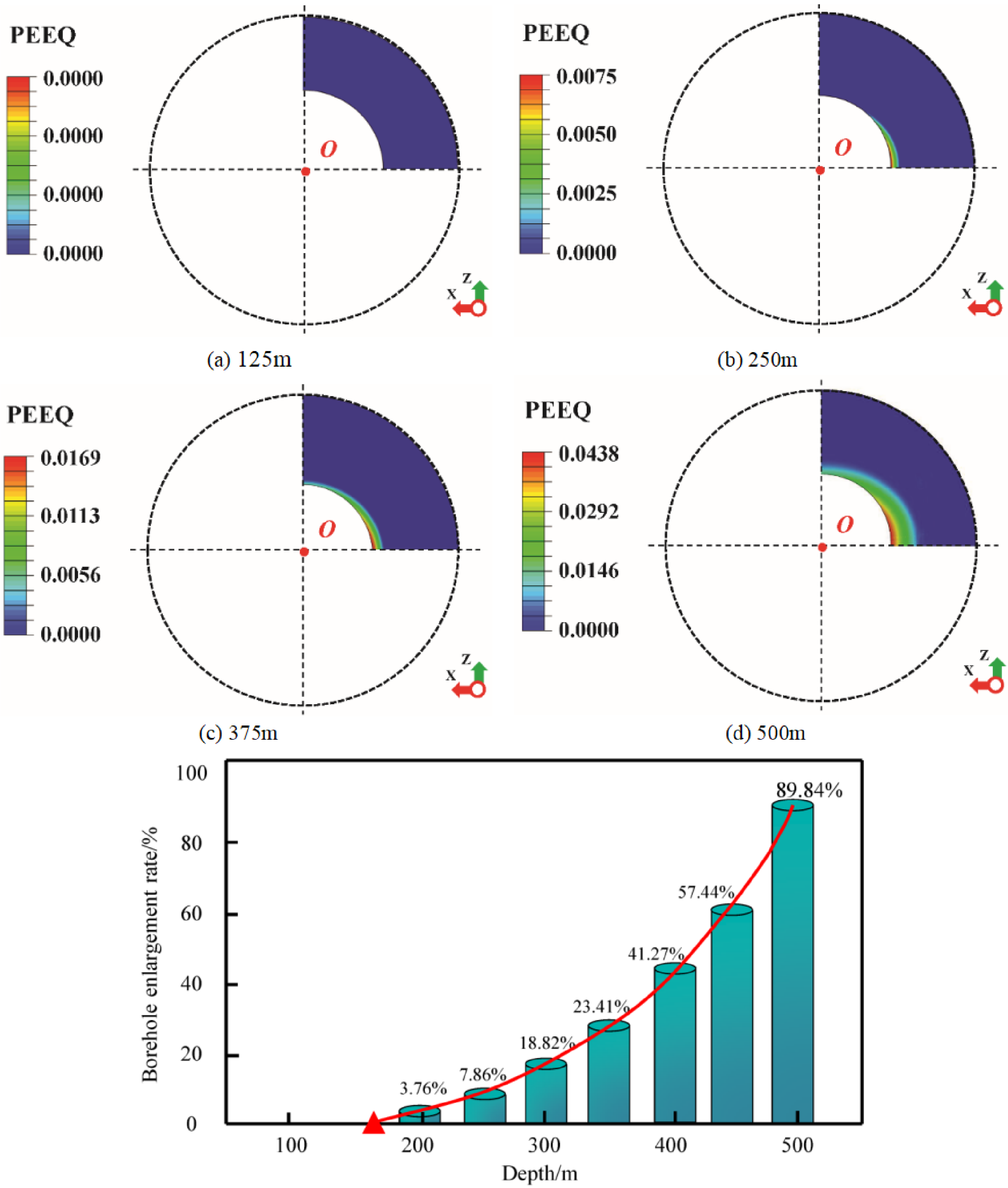

(e) Quantitative relationship between borehole enlargement rate and model depth

Figure 10. Effect of model depth on wellbore stability.

should be paid to the stability of the wellbore and sediment in deep permafrost. It is recommended

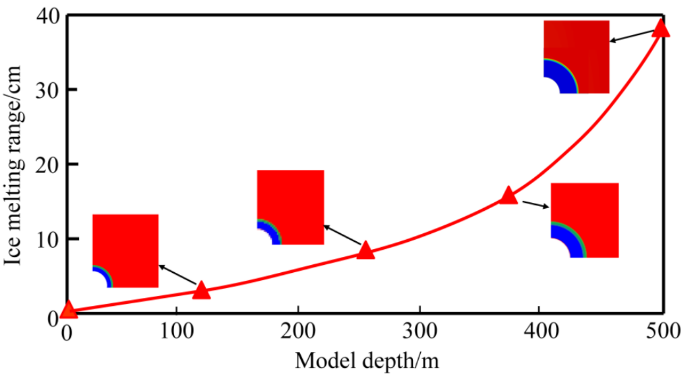

Figure 11. Distribution nephogram of ice saturation around wellbore at different model depths.

to take appropriate engineering measures to reduce potential instability risks of wellbore.

4 Effect of Engineering Conditions on Wellbore Stability

The properties of the drilling fluid (e.g., temperature, density, and salinity) can also influence wellbore stability in permafrost. In this section, the influence of the drilling properties on the wellbore stability in permafrost was explored, in order to lay a theoretical foundation for engineering designs related to drilling operations.

4.1 Drilling Mud Density

For conventional reservoirs such as shale, an important cause of borehole collapse is the insufficient drilling fluid density, which results in inadequate bottom-hole pressure to effectively support the borehole [42]. However, in temperature sensitive reservoirs such as hydrate deposits and permafrost, hydrate dissociation or ice melting leads to a decrease in sediment strength and stress relief, which exacerbates this phenomenon. Therefore, in this section, instability and collapse of vertical wellbore in permafrost were numerically studied for drilling fluid relative densities ranging from 0.98 to 1.10. Meanwhile, the corresponding mechanisms were then discussed. It should be noted that the relative density is defined with respect to a drilling fluid density with a salinity of 20 g/L.

Figures 12 and 13 present the qualitative and quantitative characterization results, respectively, of the influence of drilling fluid density on wellbore stability in permafrost. From Figures 12 and 13, it can be observed that the distribution range of PEEQ around wellbore significantly decreases with the increasing drilling fluid density. This indicates that, within the investigated density range, wellbore stability progressively improves as the drilling fluid density increases. Under underbalanced drilling conditions (i.e., when the relative mud density is below 1.0), the lower hydrostatic pressure cannot effectively support the wellbore. The melted permafrost around wellbore is prone to collapse due to stress relief, which causes borehole enlargement. In addition, due to stress sensitivity, the sediment exhibits higher permeability at lower drilling fluid densities, leading to more intense thermal convection in the near-wellbore region [43]. This leads to a wider region of ice melting around wellbore, further exacerbating wellbore stability. As observed in Figure 13, it when the relative density of the drilling fluid is 0.98, the range of ice-melting region is 32.54 cm (see Table 4), and the borehole enlargement rate reaches 89.84%. Within the lower range of fluid densities, the borehole enlargement rate decreases progressively as the drilling fluid density increases. At a relative drilling fluid density of 1.01, the borehole enlargement rate has been reduced to 57.65%.

As the drilling fluid density increases, the higher hydrostatic pressure can provide enough support to the wellbore, thereby helping to prevent severe wellbore collapse and instability. Besides, the permeability of the sediment surrounding the wellbore decreases due to the elevated stress it experiences under higher hydrostatic pressure and the associated thermal convection is weakened. In this case, ice melting range with the near-wellbore inevitably becomes narrower to some degree. When the relative density of the drilling fluid increases to 1.07, the ice-melting region has narrowed to 29.22 cm, which is only 3.32 cm less than that observed at a relative density of 0.98. As the density further increases to 1.10, the ice-melting region continues to narrow, reaching 28.56 cm. Overall, the rate at which the borehole enlargement rate decreases with increasing drilling fluid density gradually diminishes, which can be evidenced by the progressively flattening trend of the curve in Figure 13(b). When the relative fluid density increases to 1.10, the borehole enlargement rate has decreased to 2.68%. The effect of reduction in sediment strength and the stress relief induced by ice melting are largely outweighed by the stabilizing effect of the increased hydrostatic pressure, which provides sufficient support to the borehole [44].

Therefore, the drilling fluid density must be designed and optimized to ensure that it provides adequate supporting pressure, thereby preventing borehole collapse and excessive borehole enlargement.

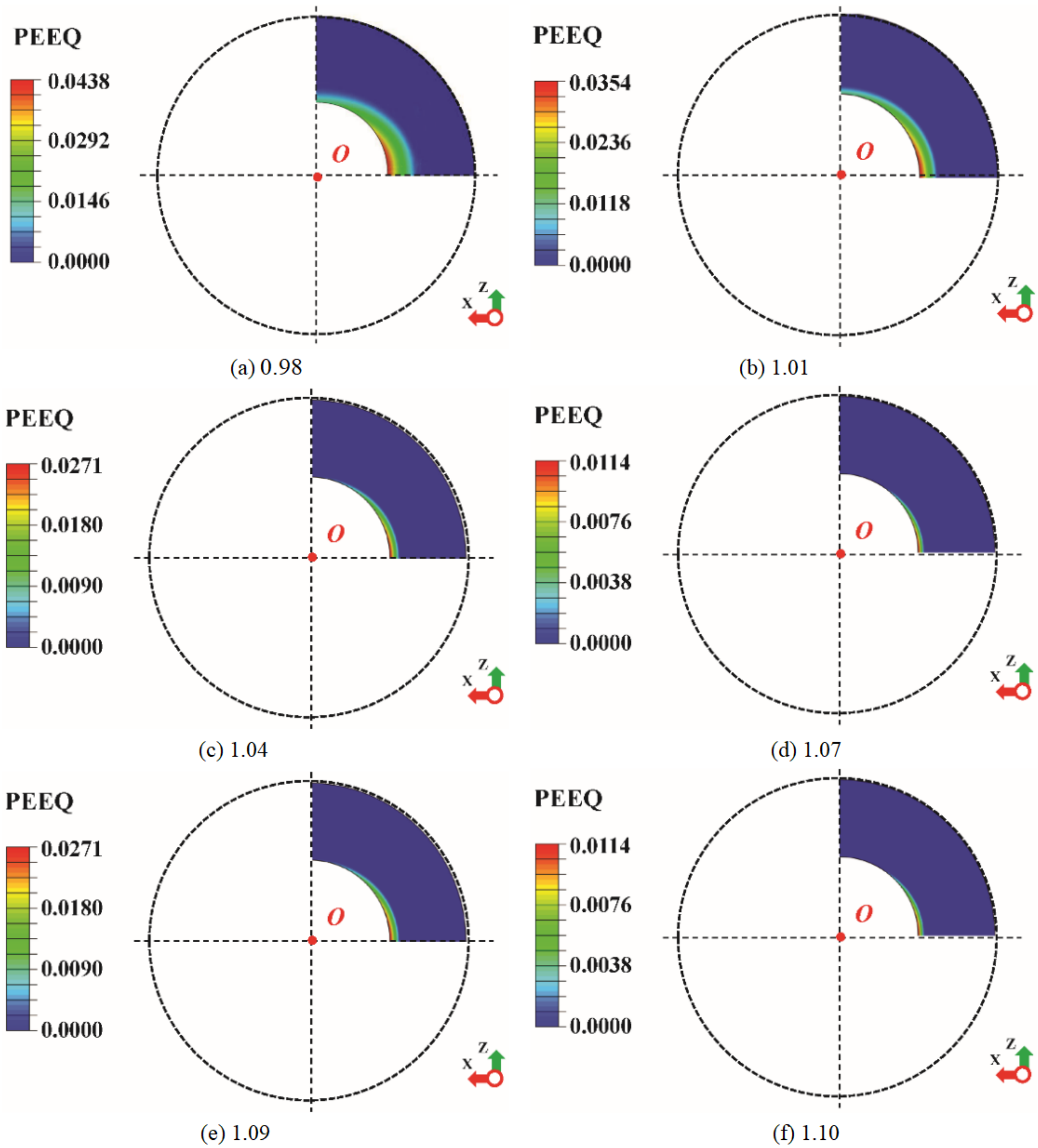

Figure 12. Nephogram of yield area around wellbore for different fluid density.

Table 4. Melting range of ice for different drilling fluid densities.

Parameter	Relative density of drilling fluid				
	0.98	1.01	1.04	1.07	1.10
Melting range/cm	32.54	31.26	30.10	29.22	28.56

Meanwhile, it should be noted that drilling fluid design must also account for the potential risk of wellbore leakage. That is to say, the density of drilling fluid designed should also not make

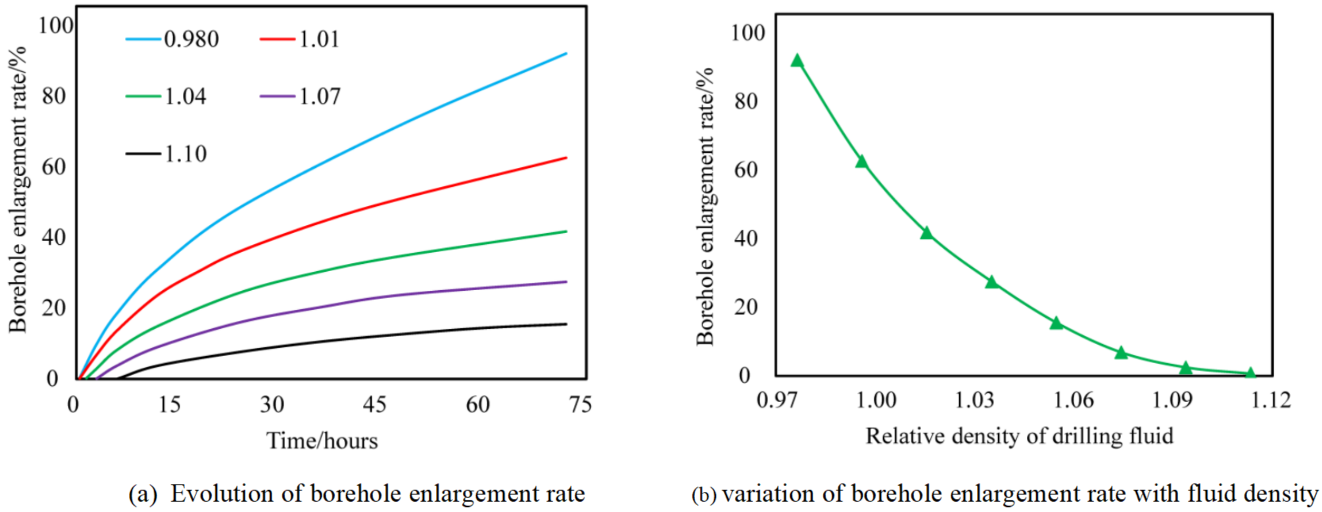

Figure 13. Quantitative relationship between borehole enlargement rate and drilling fluid density.

the bottom-hole pressure higher than the fracture pressure of permafrost. To balance the high density required for borehole collapse prevention with the leakage risk in permafrost, a strategy combining sealing and moderate density is necessary. A dense, low-permeability mud cake can be formed to effectively isolate pressure transmission and thermal invasion. In this way, wellbore stability can also be maintained at a lower equivalent circulating fluid density.

4.2 Drilling Mud Temperature

In drilling operation, the drilling fluid is jetted through the bit to clean the bottom of wellbore, and then transport the cuttings upward through the annulus by mixing with invading pore fluids [45]. Therefore, the temperature of the drilling fluid flowing in the annulus is influenced not only by the temperature of the drilling fluid in the mud pit but also by the temperature of the target formation. The influence of fluid temperature on wellbore stability was studied, and the corresponding mechanism was also explored. In this study, the drilling fluid temperature ranging from 0°C to 30°C was selected to investigate its impact on the distribution region of PEEQ around wellbore, and the results were shown in Figures 14 and 15.

To further clarify the mechanism, Table 5 summarizes the variations in heat transfer from high-temperature drilling fluid in the annulus, as well as the corresponding melting range of ice at different drilling fluid temperatures. From Figures 14 and 15, and Table 5, it can be seen that when fluid temperature is low, heat conduction is weak due to the minimal temperature difference between fluid and permafrost. In this case, stability of both ice and permafrost structure can be well maintained during the drilling process. When the temperature of the drilling fluid is 0°C, the total heat transfer obtained from the simulation results is 1.219×10^6 J. Although limited heat transfer takes place under this simulation condition, the temperature of the near-wellbore sediment remains below the melting point, and thus no ice melting is observed. At this fluid temperature, there is almost no distribution of plastic yield zones around the wellbore, and the borehole enlargement rate is only 16.17%. This observed borehole enlargement rate is attributable solely to insufficient bottom-hole pressure to support the wellbore and is unrelated to any ice melting around the wellbore. Across all drilling fluid temperatures that do not induce ice melting in the near-wellbore region, wellbore instability is governed entirely by this mechanism. When the drilling fluid temperature increased to 1.45 °C, the permafrost near the wellbore began to exhibit noticeable ice melting. Nevertheless, the borehole enlargement rate at this temperature remained unchanged at 16.17%.

As the temperature of the drilling fluid increases, the plastic yield region (i.e., PEEQ distribution region) around the wellbore expands rapidly. This markedly compromises wellbore stability and leads to a significant increase in the borehole enlargement rate. When the fluid temperature increases to 10°C, the total heat transferred in simulation reaches 6.699×10^6 J, and the ice-melting front expands to a position 12.37 cm away from wellbore. Consequently, the borehole enlargement rate rises sharply to 53.27%. If the drilling fluid temperature continues to be increases, the ice-melting region will further expand, and the borehole enlargement rate will rise

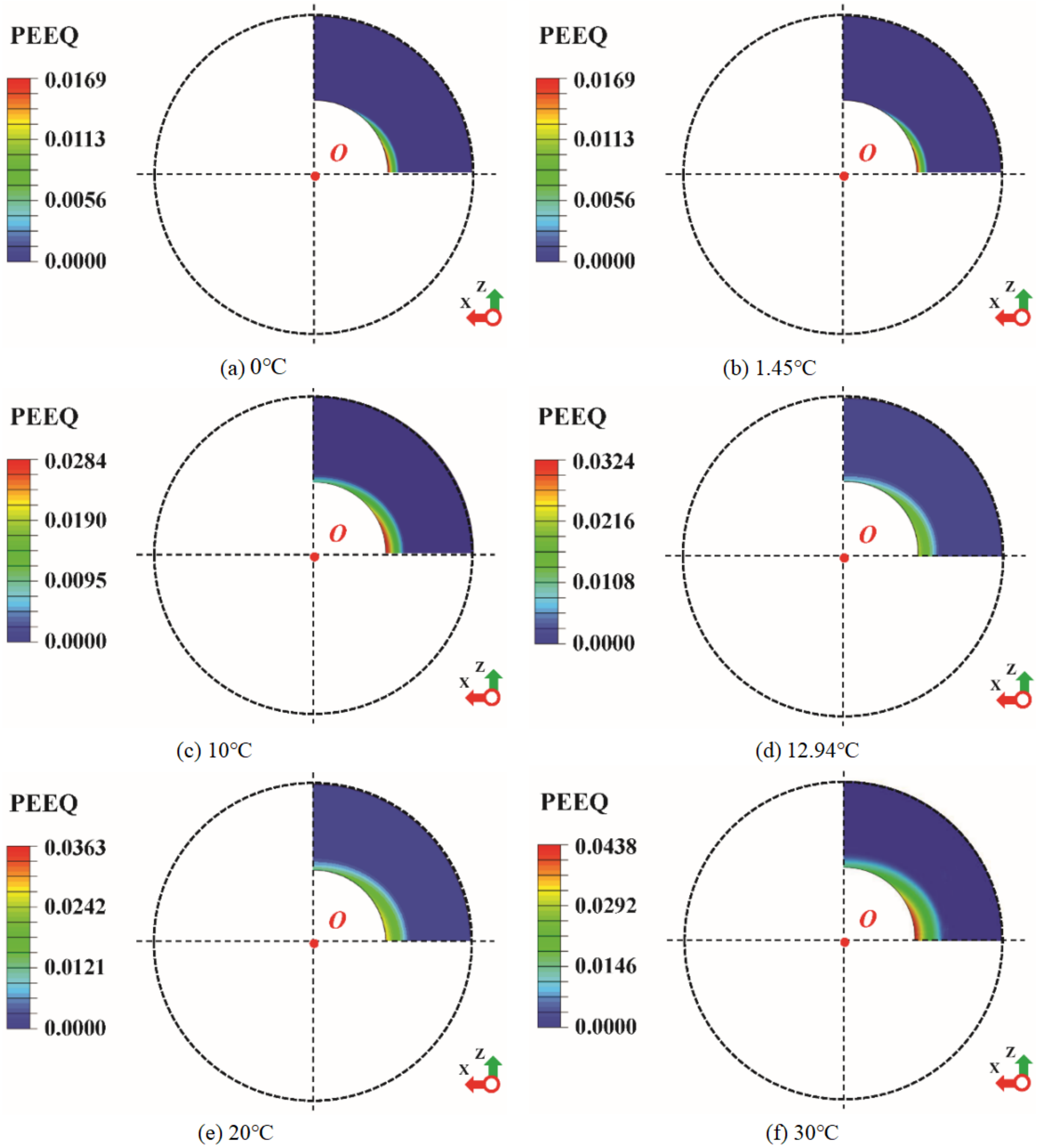

Figure 14. Nephogram of yield area around wellbore for different fluid temperature.

sharply. This rapid escalation continues until the drilling fluid temperature reaches 12.94°C. In this stage, the rapidly increasing borehole enlargement rate is attributed to the rapidly increasing heat transfer, which leads to the rapid expansion of the ice-melting region. The ice-melting range and borehole enlargement rate corresponding to a drilling fluid temperature of 12.94°C are 18.33 cm and 74.35%, respectively. If the drilling fluid temperature continues to rise beyond 12.94 °C, the rate of change in both the borehole enlargement and the surrounding yield region progressively diminishes. When the drilling fluid temperature reaches 20°C and 30°C, the borehole enlargement rate increases

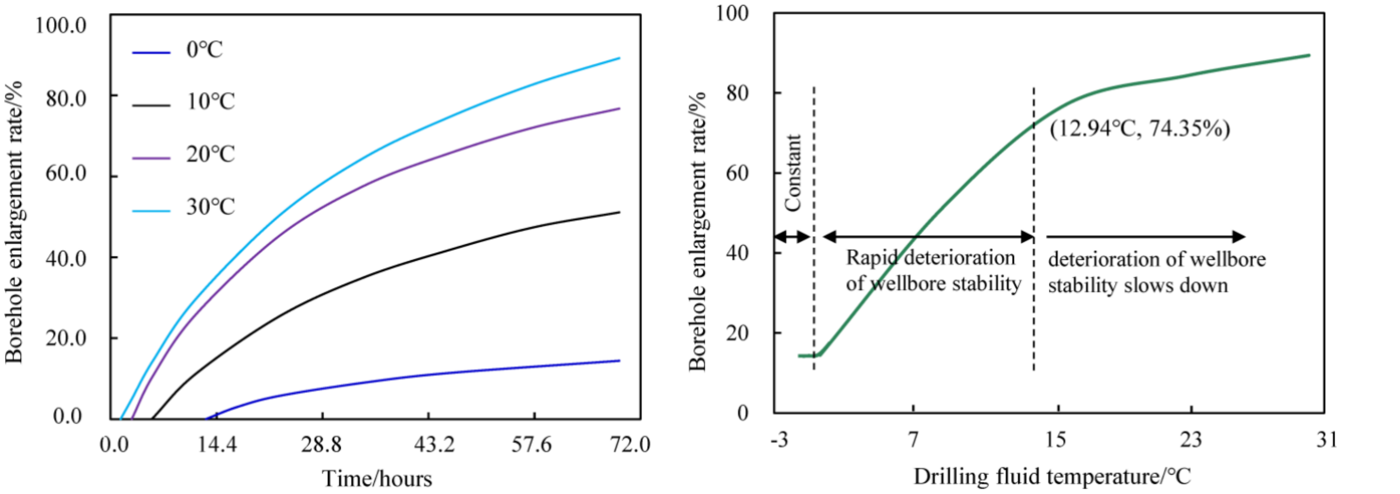

(a) Evolution of borehole enlargement rate (b) variation of borehole enlargement rate with fluid temperature

Figure 15. Quantitative relationship between borehole enlargement rate and drilling fluid temperature.

Table 5. Heat transfer and melting range of ice for different drilling fluid temperature.

Parameter	Drilling fluid temperature (°C)			
	0	10	20	30
Heat transfer, J_w	1.219×10^6	6.699×10^6	8.858×10^6	1.266×10^7
Melting range / cm	0 	12.37 	26.48 	32.54 

to 81.23% and 89.84%, respectively. The reason is that although high-temperature drilling fluid can promote ice melting over a larger area around wellbore, the accompanying heat consumption also increases substantially. This, in turn, limits the further transfer of heat and inhibits additional ice melting in regions more distant from the wellbore. Therefore, optimization of the drilling fluid temperature is critical for maintaining wellbore stability during drilling in permafrost.

4.3 Drilling Mud Salinity

The increase in the mineralization or salinity of the drilling fluid typically lowers the freezing point of water and the melting point of ice [46, 47]. This occurs because the Na^+ released from dissolved salts disrupt the hydrogen-bonding network of water molecules through hydration and electrostatic interactions. This disruption makes it more difficult for water molecules to organize into stable ice crystals. This phenomenon is known as the "freezing point depression" effect. The influence of drilling fluid salinity on the freezing point can be described by a theoretical model, expressed as:

$$\Delta T_f = K_f \cdot m \cdot i \tag{1}$$

where ΔT_f is the depression of freezing point in °C, K_f is the depression coefficient of freezing point, which is 1.86 °C·kg/mol for water. m is the molar concentration of the solute in mol/kg. i is the Van't Hoff factor, which represents the number of ions produced when an inorganic salt dissolves in water. For sodium chloride, the Van't Hoff factor is $i = 2$, as NaCl ionizes into Na^+ and Cl^- in water. However, the salinity and molar concentration of inorganic salts need to be converted in order to determine the parameter ΔT_f. Nonetheless, to determine the parameter ΔT_f, the salinity of the drilling fluid must first be converted to the corresponding molar concentration of the inorganic salts. Taking sodium chloride as an example, if the salinity of the drilling fluid is $C_{\text{NaCl}}(\text{g/L})$, its

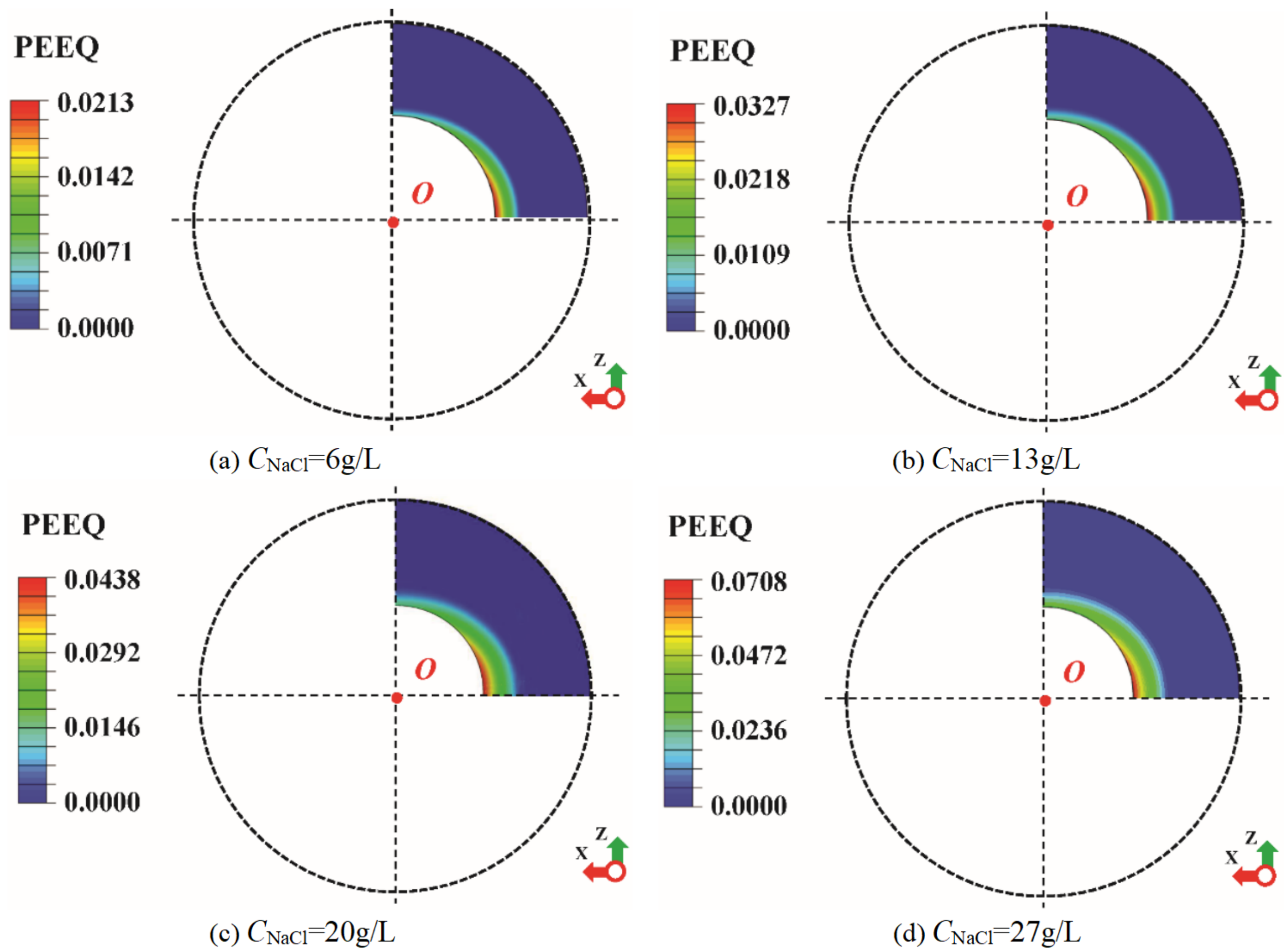

Figure 16. Nephogram of yield area around wellbore for different fluid salinity.

molar concentration can be calculated by

$$m = C_{NaCl}(g/L)/58.44.$$

Based on this, wellbore stability was investigated in this section for drilling fluid salinities of 6 g/L, 13 g/L, 20 g/L, and 27 g/L, and the instability mechanisms were also examined. The corresponding depression of freezing point for these four salinities are 0.381 °C, 0.823 °C, 1.268 °C, and 1.717 °C, respectively, as summarized in Table 6. The distribution of yield area around wellbore under different fluid salinity conditions is shown in Figure 16. Correspondingly, the relationship between borehole enlargement rate and drilling fluid salinity is quantitatively presented in Figure 17.

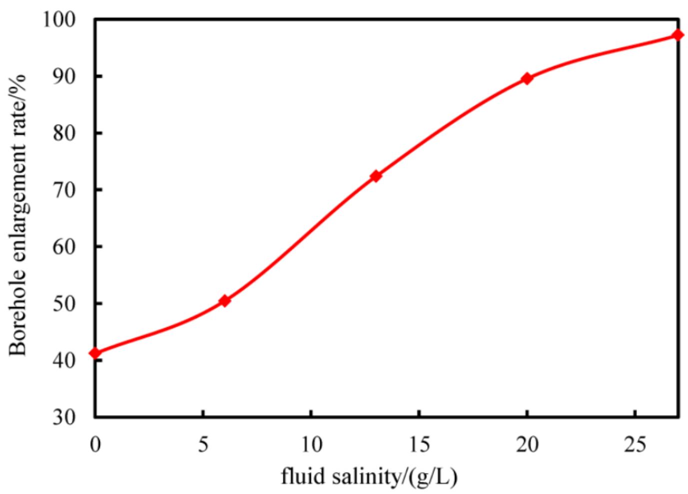

Figure 17. Relationship curve between borehole enlargement rate and fluid salinity.

As shown in Figures 16 and 17, when the drilling fluid salinity is below 6.0 g/L, the freezing-point depression effect is weak, and the ice-melting region exhibits only minor changes with salinity. As the salinity of drilling fluid increased from 0 g/L to 6.0 g/L, the final range of the ice-melting region expanded only from 17.67 cm to 20.34 cm, increasing by 15.11%. The limited change in the ice-melting region leads to a correspondingly slight variation in the borehole

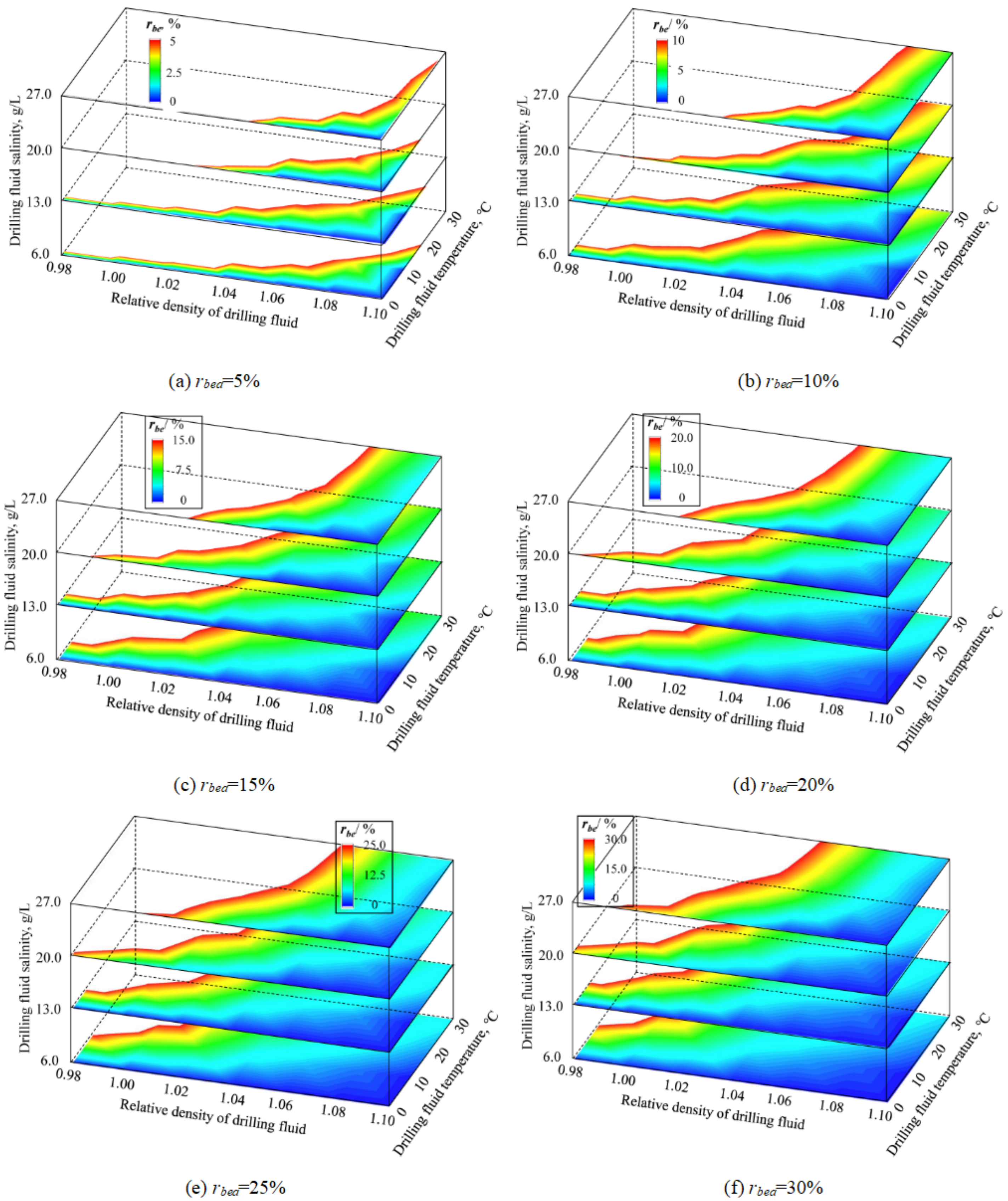

Figure 18. Recommended combinations of fluid temperature, density, and salinity when the initial ice saturation is 0.15 in permafrost.

enlargement rate within this salinity range, increasing only from 41.18% to 50.44%. However, when the

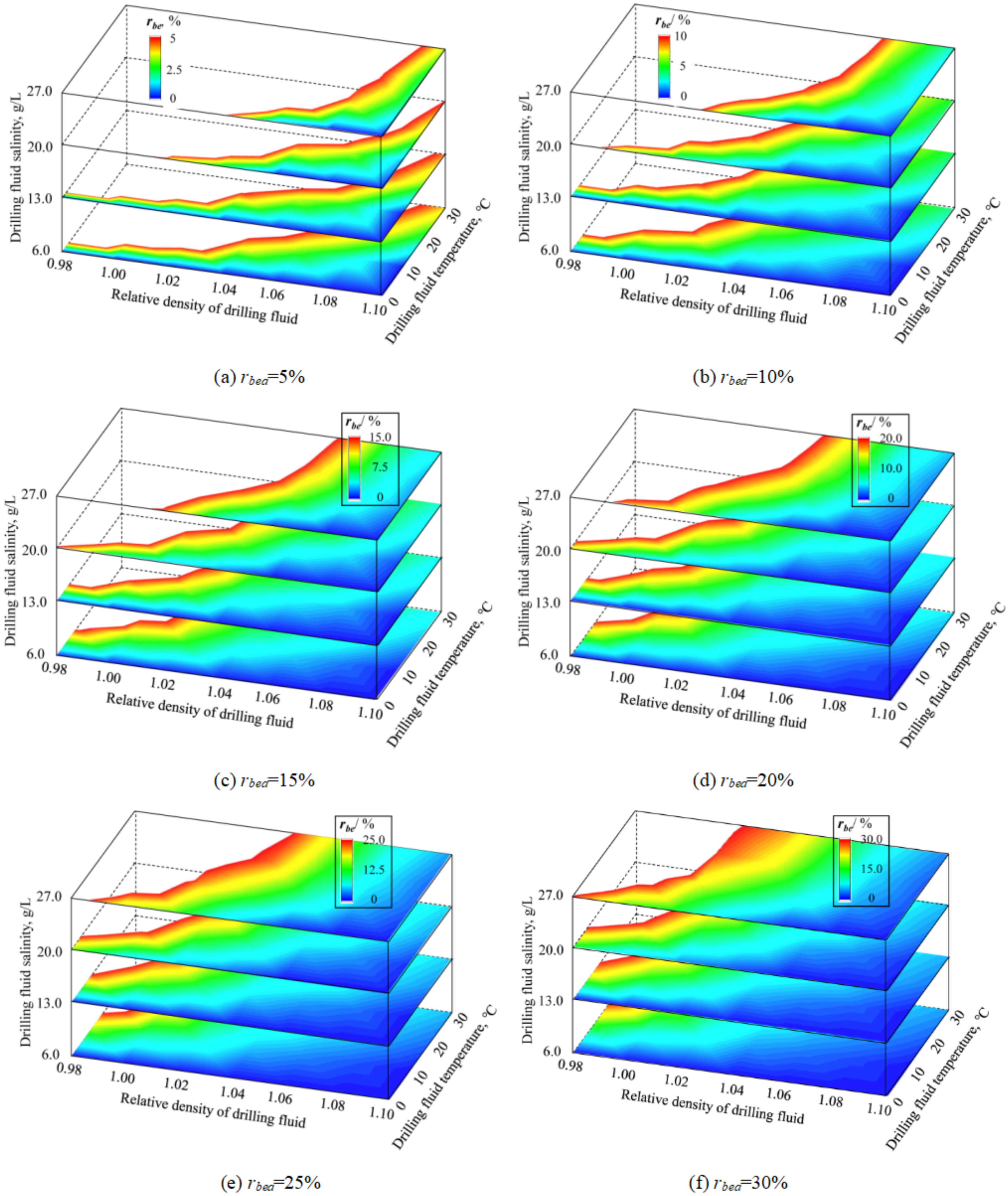

Figure 19. Recommended combinations of fluid temperature, density, and salinity when the initial ice saturation is 0.30 in permafrost.

salinity of drilling fluid exceeds $6.0\,\mathrm{g/L}$, the borehole enlargement rate increases rapidly with the increasing salinity (see Figure 17). When the drilling fluid salinity is $20.0\,\mathrm{g/L}$, the borehole enlargement rate

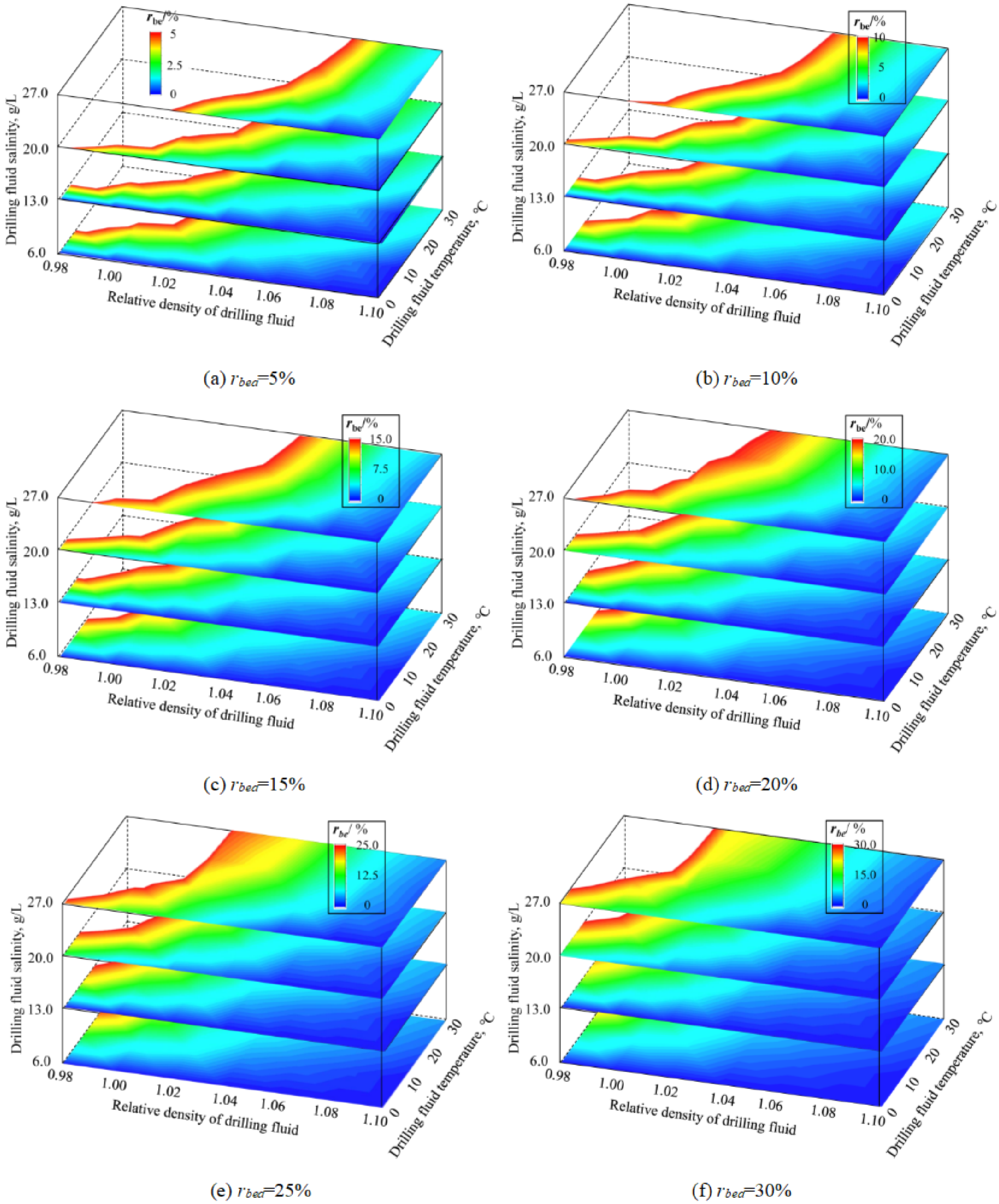

Figure 20. Recommended combinations of fluid temperature, density, and salinity when the initial ice saturation is 0.60 in permafrost.

Table 6. Melting range of ice for different drilling fluid salinity.

Parameter	Drilling fluid salinity, g/L				
	0	6	13	20	27
Melting point, °C	0	-0.381	-0.823	-1.268	-1.717
Drilling fluid density, kg/m^3	1000	1004.3	1009.3	1014.3	1019.3
Melting range, cm	17.67	20.34	27.75	32.54	34.63

rises to 89.54%. The comparison indicates that the rate of change in borehole enlargement rate (i.e., the slope of the curve) within the salinity range from $6\,\mathrm{g/L}$ to $20\,\mathrm{g/L}$ is greater than that within the range between $0\,\mathrm{g/L}$ and $6.0\,\mathrm{g/L}$. This is because the freezing-point depression effect is pronounced within this salinity range, causing a considerable expansion of the ice-melting region. Thus, the surrounding permafrost experiences both a reduction in strength and stress relief over a larger area.

Moreover, although high salinity can expand the collapse area around wellbore, its effect weakened in the high salinity range. As shown in Figures 17, when the fluid salinity exceeds $20\,\mathrm{g/L}$, the rate at which the borehole enlargement rate increases with salinity slows down. In other words, within this salinity range, the instability rate of wellbore slows down with increasing salinity. This is because, although increasing salinity raises the borehole enlargement rate by expanding the ice-melting region around wellbore, this expansion is limited. As the fluid salinity increases from $20\,\mathrm{g/L}$ to $27\,\mathrm{g/L}$, the range of ice-melting region expands by only $2.09\,\mathrm{cm}$ (see Table 6). Besides, the increase in fluid salinity slightly raises the drilling fluid density, thereby enhancing its support for the wellbore and partially counteracting the expansion of the potential collapse region.

5 Engineering Strategy for Maintaining Wellbore Stability

Wellbore stability in permafrost is influenced by both uncontrollable factors, primarily geological characteristics, and controllable factors, such as the properties of the drilling fluid. In this section, based on the simulation results of wellbore stability, the drilling fluid parameters were optimized by considering the requirements for maintaining wellbore stability. Figure 18 presents the optimized results of drilling fluid temperature, density, and salinity corresponding to different acceptable borehole enlargement rates (r_{bea}) when the initial ice saturation is 0.15. It should be noted that there are no unified requirements for maintaining wellbore stability, as it is affected by various factors, including formation properties and drilling technology. In Figure 18, the acceptable borehole enlargement rates are $5\,\%$, $10\,\%$, $15\,\%$, $20\,\%$, $25\,\%$, and $30\,\%$, respectively. The values within the colored area of Figure 18 indicate the recommended combinations of drilling fluid temperature, density, and salinity under the acceptable borehole enlargement rate. Furthermore, the data combinations located within the cool-toned regions are more strongly recommended for drilling operations in permafrost.

As shown in Figure 18, under high wellbore stability requirements (i.e. small r_{bea}), the colored area are concentrated in narrow regions with high density, low temperature, and low salinity. The narrow safe mud temperature, density, and salinity windows inevitably pose challenges and difficulties for the design and implementation of drilling operations. However, as the acceptable borehole enlargement rate increases, the colored area expands toward regions of higher salinity, higher temperature, and lower density. The proportion of this region gradually increases across the entire plotted area. This indicates that the width of the safe mud density, temperature, and salinity windows progressively widens. An increasing number of recommended combinations of drilling fluid density, temperature, and salinity are available for selection in the design of drilling operations in permafrost. This exhibits both similarities and differences compared to the design of drilling operations in conventional reservoirs, such as shale. Whether in conventional reservoirs or temperature-sensitive formations such as permafrost, as drilling requirements are relaxed, the safe mud weight window expands. However, for permafrost, both the safe mud temperature window and the safe mud salinity window also need to be accounted for in the drilling operation design.

Figure 19 and 20 present the recommended combinations of drilling fluid temperature, density, and salinity for initial ice saturations of 0.30 and 0.60, respectively. Figure 19 and 20 displays optimize patterns and results similar to those observed in Figure 18. Meanwhile, comparison of Figures 18, 19, and 20 reveals that, for consistent requirement of wellbore stability, the colored regions in Figures 19, and 20 are significantly larger than those in Figure 18. This difference indicates that permafrost with higher ice saturation contribute positively to maintaining wellbore stability during drilling. This is because high ice saturation increases the permafrost strength. As a result, it can resist a certain degree of borehole deformation and sediment yielding even under conditions of low fluid density, low temperature, and high salinity.

It should be noted that Figure 18, 19 and 20 only present the recommended combinations of drilling fluid temperature, density, and salinity for different initial ice saturation.

6 Conclusions

In the present work, factors affecting wellbore stability in permafrost were investigated, and limited engineering measures were then proposed. Based on this, the following main conclusions are obtained.

1. As the drilling operation proceeds, the advancement of the ice melting front surrounding the wellbore gradually slows down. This trend is generally consistent with the evolution of the borehole enlargement rate. Therefore, the main cause of wellbore collapse during drilling in permafrost is permafrost melting and the resulting weakening of permafrost strength, as well as stress relief within the melting region.

2. Variations in formation characteristics—such as initial ice saturation, in-situ stress differences, and permafrost depth—can all lead to differences in wellbore stability. The investigation reveals that wellbore stability improves with the increasing initial ice saturation. This is because the permafrost strength is greater, the melting range is narrower, and stress concentration is less pronounced at higher ice phase saturation. However, elevated in-situ stress anisotropy and increasing model depth both exacerbate wellbore instability. This occurs because higher in-situ stress anisotropy and greater model depth increase stress concentrations, as well as intensify ice melting in the near-wellbore region.

3. Engineering conditions, particularly the temperature, density, and salinity of the drilling fluid, also exert a substantial impact on wellbore stability when drilling through permafrost. An increase in drilling fluid temperature and salinity, coupled with a reduction in fluid density, leads to a marked worsening in wellbore stability. The impact of drilling fluid salinity on wellbore stability arises from its freezing-point depression effect, and the density of drilling fluid alters borehole enlargement rate by influencing the stress distribution around wellbore. However, thermal disturbances induced by the drilling fluid modify the temperature distribution within the permafrost, changing the conditions for ice melting and impacting the stability of the wellbore.

4. With the increasing requirements for wellbore stability, the allowable safe mud windows for density, temperature, and salinity markedly narrows, which is not conducive to the design of drilling fluid. Moreover, for permafrost with high ice saturation, the safe window for mud density, temperature, and salinity is wide, facilitating safe and efficient drilling operation. The specific design of drilling fluid temperature, salinity, and density should be determined through a comprehensive evaluation of wellbore enlargement requirements, as illustrated in Figures 18, 19, and 20.

Data Availability Statement

Data will be made available on request.

Funding

This work was supported without any funding.

Conflicts of Interest

Yinao Su is affiliated with the Research Institute of Petroleum Exploration and Development, Beijing 100083, China. The authors declare that this affiliation had no influence on the study design, data collection, analysis, interpretation, or the decision to publish, and that no other competing interests exist.

AI Use Statement

The authors declare that no generative AI was used in the preparation of this manuscript.

Ethical Approval and Consent to Participate

Not applicable.

References

[1] Zhou, X., Su, Y., Cheng, Y., & Li, Q. (2024). Evaluation of Thermal Insulation of Vacuum-Insulated Casing to Prevent Uncontrollable Melting of Ice and Borehole Instability in Permafrost. *Processes, 12*(7), 1389. [CrossRef]

[2] Li, Y., Shi, J., Cui, Q., & Song, L. (2025). Influence of Drilling Fluid Temperature, Density, and Salinity on Borehole Stability in Permafrost Strata. *Processes, 13*(2), 297. [CrossRef]

[3] Yakushev, V. (2023). Environmental and technological problems for natural gas production in permafrost regions. *Energies, 16*(11), 4522. [CrossRef]

[4] Wu, Z., Xu, L., Li, B., Wang, H., Sun, Y., & Ke, K. (2024). Hydrothermal coupling model between wellbore and permafrost for drilling in arctic cold regions. *International Journal of Heat and Mass Transfer, 235*, 126236. [CrossRef]

[5] Zhigarev, V. A. (2025). Study of the Influence of Gas-Liquid Systems on the Rate of Permafrost Thawing During Drilling. *Journal of Siberian Federal University. Engineering & Technologies, 18*(5), 574-585.

[6] Zhang, Y., Msangi, S., Edmonds, J., & Waldhoff, S. (2024). Limited increases in Arctic offshore oil and gas production with climate change and the implications for energy markets. *Scientific Reports, 14*(1), 6699. [CrossRef]

[7] Hu, X., Zhang, Y., Du Hongxing, H. Z., Wu, X., & Wang, H. (2025). Characteristic analysis of liquid CO2 jet flow field for gas hydrate well drilling. *Acta Petrolei Sinica, 46*(2), 426. [CrossRef]

[8] Wang, K. (2015). *Simulation and analysis of wellbore stability in permafrost formation with FLAC* (Master's project). University of Alaska Fairbanks. http://hdl.handle.net/11122/8866

[9] Taylor, A. E. (1979). Thermal regime modelled for drilling and producing in permafrost. *Journal of Canadian Petroleum Technology, 18*(02). [CrossRef]

[10] Pui, N. K., & Kljucec, N. M. (1978). Temperature simulation while drilling permafrost. *Journal of Canadian Petroleum Technology, 17*(02). [CrossRef]

[11] Dong, L., Wu, N., Leonenko, Y., Wan, Y., Liao, H., Hu, G., & Li, Y. (2023). A coupled thermal-hydraulic-mechanical model for drilling fluid invasion into hydrate-bearing sediments. *Energy, 278*, 127785. [CrossRef]

[12] Zhou, X., Su, Y., Cheng, Y., & Li, Q. (2024). Preliminary insight into ice melting, surface subsidence, and wellhead instability during oil and gas extraction in permafrost region. *Energies, 17*(6), 1292. [CrossRef]

[13] Lau, H. C., Zhang, M., Wang, J., & Pan, L. (2020). Some technical considerations of gas-hydrate development from chinese permafrost regions. *SPE Reservoir Evaluation & Engineering, 23*(01), 369-387. [CrossRef]

[14] Shi, J., Li, Y., Yan, C., & Xue, M. (2024). Stability Analysis of Borehole Walls When Drilling with Normal-Temperature Drilling Fluids in Permafrost Strata. *Processes, 12*(9), 1819. [CrossRef]

[15] Wang, J., Liu, L., Zhao, K., Gao, T., Liu, J., Lv, K., ... & Sun, J. (2024). Numerical simulation study on the action law of low temperature drilling fluid intrusion into rock formation in polar drilling. *Thermal Science, 28*(2 Part A), 1007-1011. [CrossRef]

[16] Kustyshev, A. V., & Leontyev, D. S. (2016). Development and research of peat drilling mud for drilling in argillaceous rocks (Russian). *Oil Industry Journal, 2016*(01), 36-38. https://onepetro.org/OIJ/article-abstract/2016/01/36/15548/

[17] Talalay, P., Hu, Z., Xu, H., Yu, D., Han, L., Han, J., & Wang, L. (2014). Environmental considerations of low-temperature drilling fluids. *Annals of Glaciology, 55*(65), 31-40. [CrossRef]

[18] Chen, F., Gao, J., Feng, Y., Lin, H., Zhang, B., Bian, G., Yang, W., & Ouyang, H. (2024). Optimizing the wellbore trajectory of directional wells considering wellbore stability Subjected to the non-independence and uncertainty of geomechanical parameters. *Geoenergy Science and Engineering, 241*, 213085. [CrossRef]

[19] Talalay, P. G. (2022). *Geotechnical and exploration drilling in the polar regions*. Springer. [CrossRef]

[20] Zhang, Y., Qiu, Z., Zhao, X., Zhong, H., Huang, W., & Mu, J. (2021). Experimental study on ultra-low temperature drilling fluid in Arctic permafrost. *Polar Science, 28*, 100645. [CrossRef]

[21] Yu, F., Guo, P., & Na, S. (2022). A framework for constructing elasto-plastic constitutive models for frozen and unfrozen soils. *International Journal for Numerical and Analytical Methods in Geomechanics, 46*(2), 436-466. [CrossRef]

[22] Allawi, R. H., & Al-Jawad, M. S. (2021). Wellbore instability management using geomechanical modeling and wellbore stability analysis for Zubair shale formation in Southern Iraq. *Journal of Petroleum Exploration and Production Technology, 11*(11), 4047-4062. [CrossRef]

[23] Jamshidi, E., Kianoush, P., Hosseini, N., & Adib, A. (2024). Scaling-up dynamic elastic logs to pseudo-static elastic moduli of rocks using a wellbore stability analysis approach in the Marun oilfield, SW Iran. *Scientific Reports, 14*(1), 19094. [CrossRef]

[24] Radwan, A. E. (2022). Drilling in complex pore pressure regimes: analysis of wellbore stability applying the depth of failure approach. *Energies, 15*(21), 7872. [CrossRef]

[25] Chen, G., Chenevert, M. E., Sharma, M. M., & Yu, M. (2003). A study of wellbore stability in shales including poroelastic, chemical, and thermal effects. *Journal of Petroleum Science and Engineering, 38*(3-4), 167-176. [CrossRef]

[26] Liao, Y., Wang, Z., Chao, M., Sun, X., Wang, J., Zhou, B.,

& Sun, B. (2021). Coupled wellbore–reservoir heat and mass transfer model for horizontal drilling through hydrate reservoir and application in wellbore stability analysis. *Journal of Natural Gas Science and Engineering, 95*, 104216. [CrossRef]

[27] Motahari, M., Hashemi, A., & Molaghab, A. (2022). Successful mechanical earth model construction and wellbore stability analysis using elastic and plasticity solutions, a case study. *Geomechanics for Energy and the Environment, 32*, 100357. [CrossRef]

[28] Ma, T., Liu, J., Fu, J., Qiu, Y., Fan, X., & Martyushev, D. A. (2025). Fully coupled thermo-hydro-mechanical model for wellbore stability analysis in deep gas-bearing unsaturated formations based on thermodynamics. *Rock Mechanics and Rock Engineering, 58*(1), 33-64. [CrossRef]

[29] Ajmera, B., & Emami Ahari, H. (2024). Review of the impact of permafrost thawing on the strength of soils. *J. Cold Reg. Eng., 38*(2), 03124001. [CrossRef]

[30] Mahetaji, M., & Brahma, J. (2024). Prediction of minimum mud weight for prevention of breakout using new 3D failure criterion to maintain wellbore stability. *Rock Mechanics and Rock Engineering, 57*(3), 2231-2252. [CrossRef]

[31] Gao, C., Miska, S., Yu, M., Dokhani, V., Ozbayoglu, E., & Takach, N. (2021). Experimental and numerical analysis of effective enhancement of wellbore stability in shales with nanoparticles. *Journal of Natural Gas Science and Engineering, 95*, 104197. [CrossRef]

[32] Hoseinpour, M., & Riahi, M. A. (2022). Determination of the mud weight window, optimum drilling trajectory, and wellbore stability using geomechanical parameters in one of the Iranian hydrocarbon reservoirs. *Journal of Petroleum Exploration and Production Technology, 12*(1), 63-82. [CrossRef]

[33] Eladj, S., Doghmane, M. Z., Lounissi, T. K., Djeddi, M., Tee, K. F., & Djezzar, S. (2022). 3D geomechanical model construction for wellbore stability analysis in Algerian Southeastern petroleum field. *Energies, 15*(20), 7455. [CrossRef]

[34] Wang, T., Yu, Y., Liu, J., Sun, Y., & Wang, Z. (2025). Risk assessment of wellbore instability during drilling in hydrate reservoirs based on thermo-hydro-mechanical coupling. *Ocean Engineering, 341*, 122689. [CrossRef]

[35] Li, H., Sun, J., Lv, K., Huang, X., Zhang, P., & Zhang, Z. (2022). Wettability alteration to maintain wellbore stability of shale formation using hydrophobic nanoparticles. *Colloids and Surfaces A: Physicochemical and Engineering Aspects, 635*, 128015. [CrossRef]

[36] Jain, G., & Singh, A. (2024). An elastoplastic semi-analytical solution for enhanced geothermal wellbore stability considering temperature-sensitive failure criterion. *Geothermics, 121*, 103046. [CrossRef]

[37] Shad, S., Kolahkaj, P., & Zivar, D. (2023). Geomechanical analysis of an oil field: Numerical study of wellbore stability and reservoir subsidence. *Petroleum Research, 8*(3), 350-359. [CrossRef]

[38] Heydari, M., Aghakhani Emamqeysi, M. R., & Sanei, M. (2022). Finite element analysis of wellbore stability and optimum drilling direction and applying NYZA method for a safe mud weight window. *Journal of Analytical and Numerical Methods in Mining Engineering, 11*(29), 67-76.

[39] Gao, L., Shi, X., Liu, J., & Chen, X. (2022). Simulation-based three-dimensional model of wellbore stability in fractured formation using discrete element method based on formation microscanner image: A case study of Tarim Basin, China. *Journal of Natural Gas Science and Engineering, 97*, 104341. [CrossRef]

[40] Lv, K., Liu, J., Jin, J., Sun, J., Huang, X., Liu, J., Guo, X., Hou, Q., Zhao, J., Liu, K., Wang, J., & Bai, Y. (2022). Synthesis of a novel cationic hydrophobic shale inhibitor with preferable wellbore stability. *Colloids and Surfaces A: Physicochemical and Engineering Aspects, 637*, 128274. [CrossRef]

[41] Li, J., Ma, Y., Liu, Y., & Liu, Q. (2024). Numerical simulation for the effect of mud cake time-dependent properties on wellbore stability. *Rock Mechanics and Rock Engineering, 57*(1), 581-596. [CrossRef]

[42] Freij-Ayoub, R., Tan, C., Clennell, B., Tohidi, B., & Yang, J. (2007). A wellbore stability model for hydrate bearing sediments. *Journal of petroleum science and engineering, 57*(1-2), 209-220. [CrossRef]

[43] Montes, A. C., Callerio, S., Turhan, Ç., Safarov, A., Ashok, P., & van Oort, E. (2024). Automatic Determination of Cuttings and Cavings Properties for Hole Cleaning and Wellbore Stability Assessment Using a Laser-Based Sensor. *SPE Journal, 29*(10), 5238-5257. [CrossRef]

[44] Liu, H., Cui, S., Meng, Y., Chen, Z., & Sun, H. (2023). Study on mechanical properties and wellbore stability of deep sandstone rock based on variable parameter MC criterion. *Geoenergy Science and Engineering, 224*, 211609. [CrossRef]

[45] Abu Dayyeh, H., Wang, X., Chen, S. L., Han, Y., & Abousleiman, Y. (2025). Graphical Analysis–Based Elastoplastic Solution for Wellbore Stability Problem in Hoek–Brown Rock under Moderate Nonhydrostatic Far-Field Stress and Undrained Conditions. *Journal of Engineering Mechanics, 151*(10), 04025055. [CrossRef]

[46] Peng, H., Yue, Y., Luo, X., Gao, J., He, M., Wen, J., Yin, H., & Chen, Y. (2023). Double-porosity poromechanical models for wellbore stability of inclined borehole drilled through the naturally fractured porous rocks. *Geoenergy Science and Engineering, 228*, 211756. [CrossRef]

[47] Li, Y., Cheng, Y., Yan, C., Xue, M., Niu, C., Gao, Y., & Wang, T. (2020). Simulating the effect of frozen soil thaw on wellhead stability during oil and gas drilling operations in arctic waters. *Journal of Cold Regions Engineering, 34*(4), 04020026. [CrossRef]

Xiaohui Zhou obtained a Bachelor's degree in Petroleum Engineering from Yangtze University and New Mexico Mining Institute in May 2015. He earned his Master's degree in Petroleum Engineering from the University of Aberdeen in November 2016. After his doctoral degree in engineering was awarded in 2025, he was appointed as a Senior Lecturer at Dongying Vocational College. His work is mainly devoted to simulations of wellbore stability in permafrost and the design and testing of insulation materials such as vacuum insulation casing. Through these studies, theoretical and technical support is expected to be provided for the efficient development of oil and gas in polar permafrost areas. (Email: 339762462@qq.com; b17020052@s.upc.edu.cn)

Feiran Yang obtained a Master's degree in Structural Geology from Southwest Petroleum University. He was appointed as a Teaching Assistant at Dongying Vocational College. He is mainly dedicated to the evaluation and analysis of unconventional oil and gas resources such as shale gas. He has participated in scientific projects such as "Analysis of National Shale Gas Resource Potential and Beneficial Prediction", and has published 5 academic papers in his research area. (Email: 331847566@qq.com)

Zhen Chen obtained a Master's degree in Engineering Management from Donghua University in May 2017. Then, he was appointed as a Teaching Assistant at Dongying Vocational College. (Email: chenzhendhu@163.com)

Yinao Su is an academician of the Chinese Academy of Engineering and currently works at the Research Institute of Petroleum Exploration and Development. He is also a doctoral supervisor at China University of Petroleum (East China) and served as the doctoral supervisor of the first author of this manuscript. He has long been engaged in the research and application of oil and gas drilling engineering technology and has profound expertise in drilling mechanics, wellbore trajectory control, and downhole tool research.